REPORT DOCUMENTATION PAGE	Form Approved OMB No. 0704-0188

1. AGENCY USE ONLY *(Leave blank)*	2. REPORT DATE	3. REPORT TYPE AND DATES COVERED
	9 Jan 97	

4. TITLE AND SUBTITLE
The Hydrogen Contribution To The Dark Matter In Draco

5. FUNDING NUMBERS

6. AUTHOR(S)
Marcus A. Boyd

7. PERFORMING ORGANIZATION NAME(S) AND ADDRESS(ES)
University of Arizona

8. PERFORMING ORGANIZATION REPORT NUMBER
96-137

9. SPONSORING/MONITORING AGENCY NAME(S) AND ADDRESS(ES)
DEPARTMENT OF THE AIR FORCE
AFIT/CIA
2950 P STREET
WPAFB OH 45433-7765

10. SPONSORING/MONITORING AGENCY REPORT NUMBER

11. SUPPLEMENTARY NOTES

12a. DISTRIBUTION AVAILABILITY STATEMENT
Unlimited

12b. DISTRIBUTION CODE

13. ABSTRACT *(Maximum 200 words)*

14. SUBJECT TERMS	15. NUMBER OF PAGES
	27
	16. PRICE CODE

17. SECURITY CLASSIFICATION OF REPORT	18. SECURITY CLASSIFICATION OF THIS PAGE	19. SECURITY CLASSIFICATION OF ABSTRACT	20. LIMITATION OF ABSTRACT

THE HYDROGEN CONTRIBUTION TO THE DARK MATTER IN DRACO

by

Capt Marcus A. Boyd, USAF

A Thesis Submitted to the Faculty of the

DEPARTMENT OF PHYSICS

In Partial Fulfillment of the Requirements

For the Degree of

MASTER OF SCIENCE

In the Graduate College

THE UNIVERSITY OF ARIZONA

1996

STATEMENT BY AUTHOR

This thesis has been submitted in partial fulfillment of requirements for an advanced degree at the University of Arizona and is deposited in the University Library to be made available to borrowers under the rules of the library. In addition, a copy is being maintained at the Air Force Institute of Technology in fulfillment of my academic agreement with the United States Air Force.

Brief quotations from this thesis are allowable without special permission, provided that accurate acknowledgment of the source is made. Requests for permission for extended quotation from or reproduction of the thesis manuscript in whole or in part may be granted by the head of the major department or the Dean of the Graduate College when in his or her judgment the proposed use of the material is in the interests of scholarship. In all other instances, however, permission must be obtained from the author or the Air Force Institute of Technology.

SIGNED: _____
MARCUS A. BOYD, Capt, USAF

APPROVAL BY THESIS DIRECTOR

This thesis has been approved on the date shown below:

_____
FULVIO MELIA, Associate Department Head
Department of Physics, University of Arizona

6/17/96
Date

ACKNOWLEDGMENTS

First and foremost, I sincerely thank my thesis advisor, Dr. Fulvio Melia. It has been an honor and a privilege to have worked with and for him. The knowledge imparted to me by him has changed my perception of the universe and has sparked my interest in a new and exciting field of science. His positive example as a diligent scientist, caring teacher, and selfless mentor has left me with a model to follow the rest of my life. Special thanks are in order for Dr. Joe Haller for his expertise and programs throughout the course of my research. Also, special thanks are in order for Dr. Robert Kurucz for his stellar model CD-ROM and Dr. Ed Olszewski for his expert advise.

I thank my wife Diana, and our daughters Lindsay and Shannon for their patience, understanding, and unconditional love during this time consuming point in my career. Though these two years in academia were challenging for us all, we managed to make it with our love for each other still strong. I apologize for all the times we did not spend together. I am in debt to you all. I also would like to thank my mother for teaching me the importance of a good education and her constant prayers during this rigorous period.

As for those in the military, I wish to thank the United States Air Force Academy Physics Department for selecting me for the opportunity to obtain a Masters of Science from the University of Arizona and having faith in me to complete the program. Also, many thanks to ROTC Detachment 20's staff and the Air Force Institute of Technology. Their administrative support, keeping me up to date on Air Force issues and sincere concerns for my family and my welfare is greatly appreciated. I would also like to thank the men and women of the Air Force for performing the daily duties I usually performed when I had a "real" Air Force job.

Last, but certainly not least, I thank God for giving me the will and strength to accomplish this goal in my life.

ABSTRACT

High-precision velocity measurements of faint individual stars in the Galactic dwarf spheroidal galaxy Draco indicate that the mass-to-light ratio in this system may be as high as ~ 100. Various possible forms of dark matter have been proposed for this class of objects, but a more recent analysis based on the Projected Mass Estimator technique seems to suggest that the non-luminous mass is distributed and may trace the stellar population. Here, we examine in detail the possible contribution of H_2 to the dark matter content of Draco and conclude that most of its mass may be in the form of $\sim 10 - 100\ M_\odot$ H_2 clouds if the typical dust grain size is at least ~ 90 times larger (i.e., $\gtrsim 48\ \mu$m) than in our galaxy. This may be consistent with the fact that the dominant dust destroying mechanisms (e.g., supernova shocks) that suppress the average grain size in the galactic plane are absent in typical dwarf Spheroidals. Thus the absence of dynamical processes (such as supernova explosions) that would normally induce massive star formation (which is non-existent in Draco) may also account for the large grain size. The lack of any observed extinction in this system would be consistent with the very low areal covering fraction ($\sim 0.1 - 1\%$) of the clouds. We show that the predicted H content in Draco is then below current 21 cm detection limits, and that even NICMOS on HST would be hard pressed to detect the prominent J and K band emission lines of excited H_2.

1. Introduction

Draco is one of the low luminosity galaxies in the vicinity of the Milky Way. The eight Galactic dwarf spheroidals (dSph) are among the lowest luminosity galaxies known, with absolute V magnitudes of, e.g., -8.9 for Draco and Ursa Minor, and -11.4 for Leo I (see Hodge 1971). Although grossly similar in stellar content to the Galactic globular clusters, their central stellar density is typically about six orders of magnitude lower. In addition, detailed studies over the past decade have revealed that dSph galaxies posses a more diverse set of properties and are comprised of more complex stellar populations than the globular cluster analogy would predict (e.g., Da Costa 1992).

It is now widely accepted that at least several members of the dSph family, including Draco, have very large mass-to-light ratios, which are deduced from high-precision velocities of faint individual stars (e.g., Aaronson & Olszewski 1987; Mateo et al. 1991). In some cases, mass-to-light ratios (M/L) from this core fitting range as high as ~ 100, much larger than those found for globular clusters and for most low-luminosity ellipticals, suggesting that many dSph satellites of our Galaxy contain dark matter. The dSphs are not rotationally supported (Paltoglou & Freeman 1987; Mateo et al. 1991), and their gas is not (yet) detectable (Knapp et al. 1978; Mould et al. 1991), making this tedious method of measuring the velocity dispersion the only kinematic technique for estimating the mass. It is now generally agreed that these kinematic studies have established the existence of dark matter within these objects. However, addressing the question of whether this matter is baryonic or nonbaryonic, and measuring its spatial distribution, has been substantially more difficult.

Although it is evident that the "large" velocity dispersions of ~ 10 km s^{-1} measured for these objects are real (as opposed to the 1 km s^{-1} value expected for M/L= 2), it has not been clear where the dark matter resides. Both halo (Pryor & Kormendy 1990; PK) and central point-like (Strobel & Lake 1994; SL) distributions have been suggested (see §3 below). Simple escape-velocity arguments show that more than 10^7 $M_\odot$ are needed to gravitationally bind all of the identified stars in the Draco system. While this simple

physical argument is in agreement with the analysis done from the velocity dispersion and King models, it has also been suggested that a single central massive black hole could provide the mass needed to explain the kinematic results. Whether or not a central cusp would be expected to form near these objects depends in part on the formation history of the dSphs. For example, if the black hole formed via accretion due to dynamical friction, the released energy would puff up the dSph and no cusp would now be present. As such, the absence of such a distribution is not necessarily conclusive evidence against the central black hole scenario.

The possibility that neutrinos might provide the missing mass in Draco (and Ursa Major) has also been considered (Gerhard & Spergel 1992), but has been ruled out on the grounds that for a reasonable neutrino mass ($m_\nu \sim 30$ eV) the required core radius (~ 10 kpc) is substantially larger ($\lesssim 1$ kpc) than the size of the dSph and the implied mass ($\sim 4 \times 10^{11}\ M_\odot$) would make the dSph's dynamical friction decay time in the Galactic halo significantly shorter than a Hubble time.

In this paper, we discuss in detail whether a significant contribution to the dark matter might be due to the presence of molecular hydrogen. An earlier search at 21 cm (Knapp, Kerr & Bowers 1978) has set a tight upper limit of about 68 $M_\odot$ on the enclosed mass of atomic hydrogen in Draco, and searches for the presence of H II regions have thus far proved inconclusive. The dSph galaxies also appear to be free of any detectable interstellar extinction due to dust. Counts of background galaxies indicate a very high degree of transparency (Hodge 1971). Our purpose here is to determine, given the physical conditions in Draco, how much molecular hydrogen could have thus far escaped detection. We begin in §§ 2 and 3 by establishing the framework for our calculations, and then develop the physical state of Draco's interior in §§4 and 5, wherein we consider the sources of ionizing and molecular dissociating radiation, and the chemical network responsible for maintaining the equilibrium populations of the various species. We describe our calculational procedure and present the results in §6, and then discuss the observational consequences in § 7, with concluding remarks in §8.

2. General Considerations

Globular clusters (to which the dSphs have sometimes been compared) appear to be devoid of interstellar matter, primarily due to the stripping of gas during their passage through the Galactic plane (occurring roughly every 10^8 years or so), and the continuous outflow of the hot interstellar matter as it is produced (Scott & Rose 1975). In the case of dSph galaxies, however, the first mechanism does not apply and the second relies on the gas temperature which may be very low. It is not unreasonable to expect that dSphs may have retained substantial quantities of primordial gas.

Recently, Elmgreen (1993) has demonstrated that the transition from H to H_2 in the interstellar medium generally depends sensitively on the pressure and radiation field, such that even a slight increase in pressure can convert a whole cloud population into H_2 molecules, whereas a slight increase in radiation can convert the clouds back to H. Almost all of the H_2 forms on the surface of dust grains, whereas its destruction is the result of radiative and collisional dissociation (Shull & Beckwith 1982). This is supported observationally by absorption line studies of H_2 regions along the line of sight to many OB stars (Rogerson et al. 1973), which have demonstrated that the fractional abundance of H_2 is determined primarily by the balance of dust versus UV radiation in the ambient medium. Molecular clouds form when the cloud column density is sufficiently high that the absorption lines become self-shielding.

The key ingredients that feature in our considerations are therefore (1) how the dark matter is distributed within Draco, i.e., what its radial profile and volume filling factor are; (2) the spectrum of the UV radiation field, which here will be a composite of components from within Draco, from the extragalactic background, and more importantly, from the Milky Way Galaxy itself; (3) the dust content; and (4) the detectable spectral signature of H and H_2. We will establish what the most likely radial distribution of the missing mass is in the following section, using the projected mass estimator (Haller & Melia 1996). The volume filling factor must be treated as a free parameter. The issue here is whether or not the gas condenses into clouds, and what their size is. In this regard, the Jeans criterion for

collapse will give some indication of the permitted range. Another indicator is provided by the required degree of shielding from the external UV radiation for the cloud interior. Since the ratio of cloud surface area to its volume scales inversely as the radius, the ratio of H to H_2 abundance will depend to some extent on the cloud size.

Establishing the dust content in Draco is much more difficult, in part because the conditions in a dSph are very different from those in the galactic interstellar medium, where we are guided by observations in inferring an average dust to gas particle number ratio of about 10^{-12} (e.g., Black & Dalgarno 1977) and a typical grain size of ~ 0.5 μm. The lack of any detectable dust (see § 1 above) is a poor guide if the areal filling factor is small. Within our galaxy, it appears that as much $\sim 0.3-0.5$ of the C, N, and O atoms, in addition to most of the heavier elements, are concentrated within the grains (Spitzer 1978). However, given the rapid rate of growth of the grain size ($\sim 2\times10^{-13}$ cm yr^{-1}), it is not yet fully understood why grains typically do not grow very much beyond ~ 0.5 μm in radius. It is likely that the mechanisms that destroy the grains are sensitive to their size. Several important examples of these are sputtering and grain-grain collisions in interstellar shocks, sputtering and sublimation in H II regions, photodesorption by UV, sputtering by cosmic rays, and sublimation during a supernova radiation pulse, which is particularly important for the more volatile mantle materials. Photodesorption and sputtering in shock waves are the principal destruction mechanisms for less volatile mantle ices. Sputtering and grain-grain collisions account for most refractory grain destruction (Draine & Salpeter 1979). Interstellar shocks are presumably much less prevalent in Draco than in typical regions of the galaxy, mainly due to the absence of supernovae and the (expected) extremely low rate of cloud-cloud collisions. In addition, the cosmic ray intensity at the location of Draco ~ 67 kpc from the galactic center is expected to be significantly lower than it is within the galaxy. This lack of any important destruction processes may lead to a growth of dust grains beyond the level seen in typical locations within our galaxy. We shall therefore treat the average grain size r_g in Draco as a parameter to be determined, and consider a range of reasonable values up to ~ 48 μm.

Closely coupled to this is the metal abundance in Draco. Using the spectral flux distributions of red giants in this system over the range $\lambda\lambda$ 3240 – 7620, Zinn (1978) concluded that the mean metal abundance [Fe/H] $= -1.86 \pm 0.09$ is actually larger than that in some of the globular clusters, such as M92. We shall adopt this value of the metallicity in our calculations and we will assume that, just like the situation in our galaxy, the dust grains in Draco contain about half of the C, N, and O atoms and most of the heavier elements.

Ultimately, the amount of H and H_2 gas must be reconciled with the available observations. In the interstellar medium, UV absorption line studies of H_2 regions are made possible by the nearby ($\lesssim 10 - 30$ pc) presence of OB stars, which act as background sources (Jura 1975). Dwarf Spheroidal galaxies are generally devoid of such UV bright stars, making this method of detection unlikely. Under normal circumstances in interstellar clouds, the temperatures are not high enough to excite molecules to vibrational or rotational states above ground. However, a substantial fraction of the molecules may be excited into vibrational or high rotational states by UV radiation (Gould & Harwit 1963), which then de-excite by emitting infrared radiation. In § 7 below, we will calculate the expected H_2 spectrum of Draco and discuss the instrument sensitivity required for a detection. The H content is already limited to less than about 68 $M_\odot$ by the available 21 cm data (see above).

3. The Dark Matter Component in Draco

a) Inferring Mass Distributions Using The Projected Mass Estimator

One can exploit a "tracer population" with observed radial velocities, v_{zi}, and projected positions, (x_i, y_i), associated with a gravitating system to infer its *total* mass using the projected mass estimator (PME) (Bahcall & Tremaine 1981 BaT; Heisler, Tremaine & Bahcall 1985 HTB). The average of the quantity ${v_{zi}}^2 \; r_{\perp i}/G$ over the whole tracer

population is related to the total mass M by

$$\frac{32}{\pi}\,\frac{1}{N}\sum_{i=1}^{N}\frac{{v_z}^2{}_i\, r_{\perp i}}{G} \;=\; \left(\frac{32}{\pi\, G}\right)\,\langle {v_z}^2\, r_\perp\rangle \;=\; CM \;\;, \qquad (1)$$

where the z-axis is oriented along the line-of-sight and $r_{\perp i}$ is the radius of tracer object i from the center of the distribution as projected onto the plane of the sky. The normalization factor, C, depends on the shape of the gravitational potential and the distribution of the orbits of the tracer population. For a Keplerian potential (i.e., a central concentrated mass), it is equal to 1, 2, or 3, when the orbital distributions of the tracer population are respectively radial, isotropic, or circular. On the other hand, when the system is self-gravitating (no point mass) the value of C is 0.5, 1, or 1.5 for the same cases of the distribution of orbits. Given N sample objects drawn from the tracer population, the fractional standard deviation of the inferred mass M is proportional to $N^{-1/2}$. This procedure has certain advantages over the virial theorem (BaT), yet one limitation is that proper motion data are generally unavailable and assumptions are necessary to constrain the value of C.

Haller and Melia (1996) showed how one could use the projected mass estimator to infer not only the total mass, but also the mass *distribution* of a gravitating system. Consider a spherically symmetric distribution of tracer objects in steady state with no rotation and a known distribution function, $f_1(\mathbf{r},\mathbf{v})$, and allow for the presence of a spherically symmetric distribution of matter due to other components, $M_2(r)$. The velocity dispersion ellipsoid for the tracer objects will be aligned with the radial coordinate basis vectors. Since the system is spherically symmetric, the transverse velocity dispersions are equal: ${\sigma_\theta}^2(r) \;=\; {\sigma_\phi}^2(r) \;\equiv\; {\sigma_t}^2(r)$. Let us define the quantity $\Lambda(r) \;\equiv\; {\sigma_t}^2(r)/{\sigma_r}^2(r)$, which describes the shape of the velocity ellipsoid as a function of radius. For a given quantity X, the expectation value $< X >$ is weighted by the volume density of the tracer population: $< X > \;=\; \int_V X\rho_1\, d\mathbf{r}/\int_V \rho_1\, d\mathbf{r}$. Thus, the quantity $\langle {v_z}^2 r_\perp\rangle$ for an arbitrarily specified volume V is given by

$$\langle {v_z}^2 r_\perp\rangle_V = \frac{\int_V {v_z}^2 r_\perp f_1(\mathbf{r},\mathbf{v})\, d\mathbf{r}\, d\mathbf{v}}{\int_V f_1(\mathbf{r},\mathbf{v})\, d\mathbf{r}\, d\mathbf{v}} = \frac{\int_V r\sin\theta\rho_1(r){\sigma_r}^2(r)[\cos^2\theta+\Lambda(r)\sin^2\theta]\, d\mathbf{r}}{\int_V \rho_1(r)\, d\mathbf{r}}. \qquad (2)$$

Using the above relation and the spherical Jeans equation, it can be shown that for a sample of tracer objects contained within a circular aperture centered on the distribution, a more general form of Eq. (1) is

$$\left(\frac{32}{\pi\, G}\right) \langle {v_z}^2 r_\perp \rangle = C' \times [< M_1(r) > \; + \; < M_2(r) > \; + M_B] \; . \tag{3}$$

The averaged quantity on the left hand side of Eq. (3) can be readily obtained from observations. If one has an underlying model of the distribution function of the tracer objects and the enclosed mass function of other components $M_2(r)$, then all of the quantities on the right hand side can be computed. Each of the terms on the right is a ratio of integrals and are functions of the projected radius R of the aperture that contains the volume V of tracer objects. We call such a sampling the "aperture PME". In the limit as $R \rightarrow \infty$ one recovers the relation given by Eq. (1).

We call the factor C' the "orbit-type" factor because it is an average of the velocity ellipsoid shape parameter $\Lambda(r)$, weighted by the radial kinetic energy density of the tracer population. As $R \rightarrow \infty$, it generalizes the factor C appearing in Eq. (1). The first term inside the brackets of Eq. (3) is a density weighted average of the enclosed mass function for the tracer population taken over the sampled volume (in this case a cylindrical volume). Similarly, the term $< M_2(r) >$ is a density weighted average of other mass components but the weighting comes from the tracer population, not the density of these other components. Finally, the last term we call the "excess measured" mass M_B. It arises because one is sampling only a finite volume and this boundary term is nonvanishing at finite radii. It may even be quite important at smaller radii. When the sampling volume is a projected cylinder, the variation of these terms with R is quite different from their variation with radial coordinate r if one were to use a spherical sampling volume.

The standard deviation of the projected mass estimator for the given sample volume is given by $N^{-1/2}(32/\pi G)\sqrt{\langle {v_z}^4 r_\perp^2 \rangle_V - (\langle {v_z}^2 r_\perp \rangle_V)^2}$, where N is the number of sampled objects. (It is assumed that the distribution of sampled objects reflects the intrinsic distribution.)

b) Application Of The Aperture PME To Draco

The dark matter distribution for Draco was modelled by PK using two-component King models (1966) to estimate the mass of a possible extended halo. An alternative model for this galaxy was proposed by SL, who assumed that the gravitational potential is dominated by a central black hole with a mass of order $10^7\ M_\odot$. These two models represent, in a way, extreme cases for the mass distribution for this galaxy. The best fitting suite of models presented by PK show that it is possible for the dark matter to be more extended than the visible population of stars. For simplicity of comparison, we restrict our attention to the PK model which assumes the dark matter is distributed in the same way as the stars and the total ratio of dark to light matter is 100. This same M/L ratio is also assumed for the model proposed by SL.

For a King model, the gravitational potential ψ and energy per unit mass E are customarily measured relative to the tidal radius r_t of the system:

$$\psi \equiv -U + U_0 \quad \text{and} \quad \epsilon \equiv -E + U_0 \quad \text{for} \quad U_0 = -\frac{M(r_t)}{r_t}. \tag{4}$$

The distribution function of the tracer stars is taken to be a truncated Maxwellian given by

$$f_1(\epsilon) = (2\pi\sigma_K^2)^{-\frac{3}{2}}\,(e^{\epsilon/\sigma_K^2} - 1) \qquad \epsilon > 0, \tag{5}$$

while $f_1(\epsilon) = 0$ for $\epsilon \leq 0$. For units such that the scale radius r_0, G, and central density, ρ_0, are unity, then the square of the scale velocity σ_K^2 has a dimensionless value of $4\pi/9$.

The local density is a function of the local potential ψ via an integration of Eq. (5) over all velocities up to the escape velocity, $\sqrt{2\psi}$. The one-dimensional velocity dispersion $\sigma^2(r)$ is also computable (see BT, p.235). Choosing a ratio ψ_0/σ_K^2, and setting its initial gradient $d\psi/dr = 0$, Poisson's equation is integrated to obtain the functions $\psi(r)$, $\rho_1(r)$, and $M_1(r)$. The King model parameters obtained by PK to fit the Draco system are $\psi_0/\sigma_K^2 = 3.15$, scale radius $r_0 = 156$ pc, and scale velocity $\sigma_K = 11.4$ km sec^{-1}.

Strobel and Lake (1994) proposed a distribution function of tracer stars that resulted from the formation of a massive black hole of order $10^7\ M_\odot$ from a primordial isothermal

distribution of stars with uniform density ρ_0 and one-dimensional velocity dispersion σ_v. As the black hole formed, the stellar distribution function was an adiabatic invariant (Young 1980) and those stars that remained bound to it had initial energies $E_i << {\sigma_v}^2$ which results in the distribution function

$$f(E) = \frac{\rho_0}{(2\pi {\sigma_v}^2)^{3/2}}. \tag{6}$$

SL set $\sigma_v = 3$ km sec^{-1} based on the typical velocity dispersion of Galactic globular clusters. The density of stars is then found by integrating the distribution function in Eq. (6) over all velocities up to the escape velocity at each radius, while the velocity dispersion (assumed to be isotropic) ${\sigma_v}^2(r)$ is also an analytic function. By fitting the projected surface density and velocity dispersion profiles, they obtained a tidal radius for Draco of $r_t = 720$ pc and a central black hole mass $M_\bullet \approx (1.5 - 2.0) \times 10^7\ M_\odot$.

To test which of these models is better able to account for the stellar velocity data, we computed the aperture PME as a function of R using the best fitting parameter values given by these workers. The resulting aperture PME curves were then compared with the radial velocity data set of Olszewski (1994) (Figure 1). Although the statistical errors are large, the case for an extended dark matter distribution in Draco seems more favorable. In particular, if a central point mass were dominating the gravitational potential for this system then one would not expect the PME to decrease so strongly as $R \rightarrow 0$. Generic models that incorporate a massive black hole as the dominant mass component all have a high value for the aperture PME when the radius of the sample aperture is less than the size of the core radius of the tracer population (Haller & Melia 1996). On the basis of these results, we conclude that the dark matter in Draco is most likely distributed, and may in fact trace the luminous matter. In Figures 2 and 3, we show, respectively, the dark mass density distribution for the best fit PK model (see above) and the corresponding scales of velocity.

4. The Radiation Field

The radiation field within Draco is produced primarily by (i) its stellar content, (ii)

the extragalactic background and (iii) the stars within our own galaxy. Although these sources emit radiation across a broad spectral range, the primary band of radiation that severely affects the detectability, the structure and the composition of a typical gas cloud is the far-ultraviolet band (FUV). This band has a wavelength range of $900-3000$ $\AA$ and is responsible for the excitation, the photodissociation and ionization of important molecular species. Also, it is responsible for the excitation and ionization of some atomic species. Specifically, when hydrogen in atomic (H I) and molecular (H_2) form are the dominant species (which is usually the case for galactic gas clouds with a cosmic abundance), it is the Lyman and Werner bands ($912-1108$ $\AA$) that are the most important (Shull & Beckwith 1982; Black & VanDishoeck 1987; Martin, Hurwitz & Bowyer 1990; Sternberg & Dalgarno 1989) since H_2 is primarily excited and dissociated to form H I by FUV photons in these bands. Excitation occurs initially by a Lyman or Werner band photon exciting H_2 from its ground electron state, $X^1\Sigma_g^+$, to a higher electron state of $B^1\Sigma_u^+$ (for Lyman) or $C^1\Pi_u$ (for Werner). This stage of the excitation process is followed by a fluorescence 90% of the time to a bound vibrational-rotational excited ground electron state of H_2. For the remaining 10% of the time, dissociation occurs by H_2 fluorescence to a vibrational continuum ground state to form H I (Black & VanDishoeck 1987; Martin, Hurwitz & Bowyer 1990).

The FUV radiation field due to the stellar content of Draco itself may be safely assumed to be negligible compared to the other sources of FUV photons impingent on Draco from outside the dwarf Spheroidal Galaxy. The primary argument for this is that the stellar content of Draco is heavily biased away from stars producing FUV radiation. FUV producing stars are primarily those with a MK spectral type of O, B or A. Observations of dwarf Spheroidals (dSph) indicate that these types of stars are extremely rare in these systems and might only exist on the blue portion of the horizontal branch of a dSph's color magnitude diagram (Olszewski 1994). This is clearly evident on the horizontal branch of the color magnitude diagram constructed for Draco by Stetson (1980). From this portion of the diagram, only 2 out of 365 stars used to produce the diagram may be considered early to late A type and none are O or B type stars. The only candidate for an O or B

type star on the entire diagram is a peculiar star off the principal sequence, but it is at most an extreme late B type.

The extragalactic background is primarily produced by distant galaxies, quasars and the intergalactic medium (Paresce & Jakobsen 1980). The extragalactic FUV background has been investigated in detail by Martin, Hurwitz & Bowyer (1991), who report an upper limit to its intensity of 280 ± 35 photons cm^{-2} s^{-1} $\mathring{A}^{-1}$ sr^{-1} within a band of $1400 - 1900$ $\mathring{A}$. Assuming the background intensity to be isotropic within Draco and conservatively taking the upper limit, we estimate a total flux of $\lesssim 3.6 \times 10^{-9}$ photons cm^{-2} s^{-1} Hz^{-1} within this band. As we shall see below, this component of the FUV radiation within Draco is also negligible compared to the contribution from the Milky Way, and it may therefore itself be safely ignored.

To calculate the flux of FUV photons from our galaxy, we have developed a simple, yet fairly accurate, model of the galactic sources to produce the spectrum observed at Draco (Figure 4). This model consists of the various spectral types and luminosity classes of stars arranged uniformly on a thin plane which we call the stellar disk. The stellar spectral types range from O5 to M5 and the luminosity classes span the range from the main sequence to the super giant branch. The radius of the stellar disk is taken to be 15 kpc (Allen 1973). For the purpose of incorporating the effects of line-of-sight attenuation, we surround the stellar disk with a thicker disk of dust, which is also distributed uniformly. Its thickness is taken to be 300 pc, in agreement with the effective thickness of our galaxy for interstellar absorption. Relative to this galactic plane, Draco lies at a heliocentric distance of 67 kpc (Hodge 1971), a galactic latitude of 35 degrees, and a galactic longitude of 86 degrees. Assuming a distance of 8.5 kpc to the Galactic center, this yields about the same distance (≈ 67 kpc) from Draco to the center of our galaxy.

The integrated galactic spectrum is assembled from the spectra of individual types of stars. This is done by binning the stars within our galaxy into a MK spectral type of O5, B0, B5, A0, A5, F0, F5, G0, G5, K0, K5, M0 or M5 within a luminosity class of super giant, giant or main sequence. For simplicity, white dwarfs and sub dwarfs are classified

as main sequence stars, and sub-giants are assumed to be giants and bright giants are assumed to be super giants. Based on the available data (e.g., Mihalas & Binney 1981; Allen 1973), an average effective temperature (T_{eff}), surface gravity (g) and radius (R_s) may be assigned to each spectral type. With these, and the assumption of solar metallicity, we can then choose among the Kurucz (1993) stellar atmosphere model spectra for each stellar type, taking the closest match between T_{eff} and g. Tables 1A, 1B, and 1C show the different parameters used for each model and their originally assigned values.

To determine the number of stars within each type, we assume a total galactic stellar content of $\sim 1 \times 10^{11}$ stars and then use the luminosity functions in Bahcall's (1986) galaxy model to determine the number of stars at each absolute visual magnitude. These luminosity functions consist of a disk and spheroidal distributions with an absolute visual magnitude ranging from -7 to 16 in each case. The use of these luminosity functions has been validated recently by the demonstration that they agree very well with observational data taken with the Hubble telescope (Bahcall & Maoz 1993). The total luminosity function for the stellar disk is taken to be the sum of these two distributions at each of the corresponding magnitudes. Merging this total luminosity function with a spectral type distribution (e.g., Allen 1973, corrected by Bahcall & Soneira 1981) covering an absolute visual magnitude range between -7 and 16, it is straightforward to derive a spectral luminosity function from which we infer the percentages of each spectral type. The different spectral types are then categorized according to their visual magnitude using data provided for each luminosity class in Allen (1973), and Mihalas & Binney (1981). From this categorization, and assuming that the percentages increase logarithmically from O5 to B5, and adjusting the percentages of A0 and A5 stars to match the HR diagram of the solar neighborhood, we infer the percentage of each spectral type for a given luminosity class as shown in Figure 5 (see also Tables 2A, 2B, and 2C).

The attenuation due to dust and gas is calculated by using the average interstellar attenuation curve of Savage & Mathis (1979), which is shown in Figure 6. Here, R_λ is the ratio of the magnitude of attenuation A_λ at a certain wavelength to $E(B-V)$. We note,

however, that the dust within the galaxy is patchy, and one can at best therefore only determine the average value of $E(B-V)$, and hence A_λ. We do this by determining the average distance traversed by a path through the disk of dust from sources in the stellar disk toward Draco. Then, by assuming a visual attenuation rate of 1.9 mag/kpc (Allen 1973) and R_v of 3.2 (Mihalas & Binney 1981), we infer an average value of $E(B-V)$ equal to 0.156 by multiplying the average distance with the visual attenuation rate and dividing by R_v. This average $E(B-V)$ yields the magnitude of the attenuation at each given wavelength. We also assume that all the radiation with a wavelength less than 912 $\AA$ (i.e., the Lyman limit) does not escape from the galaxy.

The total FUV spectrum at Draco is the sum of the spectrum from each star at a distance of 67 kpc from the stellar disk, attenuated by the factor derived above. The result is shown in Figures 7 and 8 in units of photons cm^{-2} s^{-1} Hz^{-1} and photons cm^{-2} s^{-1} $\AA^{-1}$, respectively. It is evident that the FUV flux produced at Draco by the Milky Way easily dominates over the contributions from the extragalactic background and stars within Draco itself. In Figure 9, we compare our spectrum with those calculated and observed for the interstellar medium, which are expected to show a similarity in the gross features, though perhaps not in the details and in the overall flux level. The theoretical spectrum calculated by Habing (1968) is valid over the wavelength range $912-3000$ $\AA$. The long-dashed curve in Figure 9 shows his spectrum multiplied by a factor of 1.6, which accounts for the effects of a different distance and attenuation between our geometry and his. Draine's (1978) spectrum for the wavelength band of $912-2000$ $\AA$ is based on the compilation of observational and theoretical data. Our spectrum agrees quite well with his within this wavelength range if we multiply his flux by a factor of 1.7 (short dashed curve), again accounting for the different geometries in the two cases.

5. The Interaction Network

If the dark matter in Draco is baryonic—whether distributed continuously throughout the system, or composed of many small cloud constituents—it is subject to several

key chemical interactions, which we here describe. In the interest of keeping our calculations simple yet accurate, we have chosen to use elements, species and reactions based on those seen to dominate in typical interstellar clouds. Our network is therefore primarily composed of the reactions and elements used by Roberge (1981). Even though this network is relatively simple, it produces results that generally agree with the more elaborate chemical network of Black and Dalgarno (1977). We also use some components of the detailed chemical networks employed by VanDishoeck and Black (1986), and Tielens and Hollenbach (1985).

Our simple chemical network is composed of the elements: hydrogen, helium, carbon, nitrogen, oxygen, iron, silicon, sulfur and magnesium. These elements are used in 70 different reactions to produce and destroy a total of 32 different species, which include: H, He, C, N, O, Si, S, Mg, Fe, free electrons, H_2, OH, CO, O_2, H_2O, H^+, He^+, C^+, N^+, O^+, Si^+, S^+, Mg^+, Fe^+, H_2^+, OH^+, CO^+, H_2O^+, HCO^+, H_3^+, H_3O^+ and H_2^* (i.e., the vibrational-rotationally excited ground electron state of H_2). A complete list of the reactions employed in these calculations is given in Table 3.

The reactions of our network can be classified as positive ion (PI); neutral (NR); electron recombination (EI); radiative electron recombination (AI); cosmic ray (CR); photoionization and dissociation (PP); hydrogen-grain (H2) and rotational-vibrationally excited hydrogen (MH) reactions with a characteristic associated rate specific for each reaction. These rates are generally dependent on parameters such as the cloud temperature, FUV flux, line and continuum attenuation of the FUV flux and the intensity of cosmic rays within the dwarf Spheroidal galaxy. To reflect the importance of each of these parameters Table 3 also lists the rate coefficients for each reaction. The rates per particle number density for the PI, NR, EI and AI reactions, which are primarily governed by the cloud temperature, can all be calculated with the equation

$$k = A\,(T/300\ \mathrm{K})^{\alpha}\ \exp(-\beta/T)\ \ \mathrm{cm}^3\ \mathrm{s}^{-1}\ , \tag{7}$$

where T is the temperature of the cloud in Kelvins and A, α and β are the rate coefficients

for each specific reaction. As for the CR reactions, their rate is given by

$$k = \zeta\, A\,, \tag{8}$$

where A is the rate coefficient for each specific reaction and $\zeta = 1.3 \times 10^{-17}$ s^{-1} for conditions in the interstellar medium. We expect ζ to be much smaller within Draco. The rates for the PP reactions are based on a plane parallel assumption for the radiation transfer and an interstellar FUV flux following Habing (1968):

$$k = A\, S_{flux}\, \exp(-\beta\, A_v)\ \text{s}^{-1}\,, \tag{9}$$

where A_v is the visual extinction, which increases with depth into the cloud, and is primarily due to dust or other continuum extinction processes. A and β are rate coefficients for each specific reaction, and the parameter S_{flux} is a factor that scales the level of FUV flux within Draco relative to Habing's results for the interstellar medium (see § 4 above). This simple scaling is possible because the rates are directly proportional to this flux.

The rate coefficients, A, α and β in each of the above rate equations were derived by Prasad & Huntress (1980) based on theoretical and empirical results and are included in Table 3 for every reaction. This dependence on the extinction is based on empirical fits to observations along lines of sight within the galactic plane. If the typical grain size in Draco is bigger than that within our Galaxy, then the extinction law must be modified. It is beyond the scope of the work reported here to reproduce in detail an attenuation curve for a variety of dust grain distributions analogous to that shown for the ISM in Figure 6. Instead, we shall try to obtain qualitative results by assuming that the attenuation may still be written in terms of A_v with the rate coefficients as shown, though the dependence of A_v on the dust constituents is modified by the different grain radius r_g. When compared with the visual extinction in the Galaxy, the value of A_v in Draco will be enhanced by a factor $(r_g/0.5\ \mu\text{m})^2$ corresponding to the grain cross section, and a factor $(0.5\ \mu\text{m}/r_g)^3$ for the grain number density, under the assumption that the total amount of C, O, and N content of the grains is fixed to be about half of the observed abundance in this system

and that most of the heavier elements are contained therein (see § 2 above). For simplicity, we shall also assume that the optical efficiency in the wavelength range of interest scales approximately as $(r_g/0.5\ \mu\mathrm{m})^4$. This treatement of the dust attenuation will be improved in future work.

In this network, we concentrate our efforts on the species of H, H_2 and H_2^* since these are the most abundant and therefore the most likely to be detectable at the distance of Draco. This entails a detailed investigation of the formation and destruction of H, H_2 and H_2^* and their effect on other species within the cloud. One primary process for forming H_2^* is the absorption of a Lyman or Werner band photon which initially excites H_2 from its ground electron state, $X^1\Sigma_g^+$, to a higher electron state of $B^1\Sigma_u^+$ (for Lyman) or $C^1\Pi_u$ (for Werner), followed by a fluorescence to a bound vibrational-rotationally excited ground electron state, H_2^* (Black & VanDishoeck 1987; Martin, Hurwitz & Bowyer 1990). This reaction is listed as item MH14 in Table 3E and its rate is given by Tielens & Hollenbach (1985) as

$$k = 3.06 \times 10^{-10}\, S_{flux}\, \beta(\tau)\, \exp(-2.5\, A_v)\ \ \mathrm{s}^{-1}\ . \tag{10}$$

This rate takes into account the continuum attenuation due to dust through the visual extinction A_v which, again, increases with depth into the cloud and is modified from its galactic value as described above. Using the factor $\beta(\tau)$, this rate equation also takes into account the H_2 line self-shielding of the Lyman and Werner band photons. When photon absorption is dominated by the Doppler cores or the Lorentz wings ($\tau > 10$), the H_2 line self-shielding factor is given by

$$\beta(\tau) = \{\tau^{-1}\,[\ln(\tau/\pi^{1/2})]^{-1/2} + (b/\tau)^{1/2}\}\,\mathrm{erfc}(\tau b \pi^{-1} v_1^{-2})^{1/2}\ , \tag{11}$$

where the dimensionless parameters b, v_1 and τ are given by $b = 9.2 \times 10^{-3}\, \delta v_d^{-1}$, $v_1 = 5 \times 10^2\ \delta v_d^{-1}$, $\tau = 1.2 \times 10^{-14}\, N(H_2)\, \delta v_d^{-1}$, and δv_d equals the turbulent Doppler line width in km s^{-1} and $N(H_2)$ is the column density of H_2. For the linear part of the curve of growth ($\tau \leq 10$), the H_2 line self-shielding factor is given by

$$\beta(\tau) = \Sigma(-1)^n\, \tau^n/[n!(n+1)^{1/2}\, \pi^{n/2}]\ , \tag{12}$$

where the summation is over n from 0 to ∞. Since $\beta(\tau)$ is inversely proportional to τ, which is directly proportional to $N(H_2)$, it decreases with depth into the cloud. As with the PP reactions, S_{flux} is the factor that scales the FUV flux relative to that used by Habing (1968).

Black & VanDishoeck (1987) have shown that another source for producing H_2^* is the merging of two hydrogen atoms on a dust grain. When the grain number density is 1×10^{-12} times the number density of hydrogen nuclei (n_h)—a typical value in the interstellar medium—the rate for this reaction is

$$k = 3 \times 10^{-18} T^{1/2} \, y_f \, n_h \, n(H) \ \text{cm}^{-3} \ \text{s}^{-1} \ , \tag{13}$$

where y_f is the efficiency parameter (usually ≈ 3) and $n(H)$ is the number density of H.

The destruction of H_2^* is primarily due to de-excitation by the spontaneous emission of infrared radiation, collisions and reactions with other species, and the absorption of a FUV photon. The rates per particle number density for most of these reactions are based on the rate coefficients reported by Tielens & Hollenbach (1985) (see Table 3), and are given by

$$k = A(T/300 \ \text{K})^{\alpha} \exp(-\beta/T) \ \text{cm}^3 \ \text{s}^{-1} \ . \tag{14}$$

The peculiar rate of reaction MH3 (involving H_2^* and H_2) and that of reaction MH1 (the absorption of a FUV photon) are also given by Tielens & Hollenbach (1985) as

$$k = 1.4 \times 10^{-12} \, T^{1/2} \exp[-18100/(T + 1200)] \ \text{cm}^3 \ \text{s}^{-1} \ , \tag{15}$$

and

$$k = 1.0 \times 10^{-11} \, S_{flux} \exp(-2.5 \, A_v) \ \text{s}^{-1} \ , \tag{16}$$

respectively.

H_2 is formed by many process, as is evident from the network of reactions listed in Table 3, but it is its destruction by a Lyman or Werner band photon that affects its population the most. And when H_2 is a dominant species in a cloud, this destruction process is the

main source for producing H. The rate for this reaction is given by Tielens & Hollenbach (1985) as

$$k = 3.4 \times 10^{-11}\, S_{flux}\, \beta(\tau)\, \exp(-2.5\, A_v)\ \ \mathrm{s}^{-1}\ , \qquad (17)$$

where again the shielding factor $\beta(\tau)$ is used.

6. Calculational Procedure and Results

The dark matter distribution we derived in § 3 above specifies the average density (or equivalently, the enclosed mass) as a function of radius. Its clumpiness, however, is not known. We shall therefore consider two extreme cases, one in which the matter is distributed continuously throughout the dSph (i.e., no clumpiness), and a second in which the gas is condensed into $M_c = 10\ M_\odot$ clouds. A more general profile, constituting a range of cloud sizes and masses will be left to future work.

In both cases, the cloud temperature T is assumed to be the representative value of 100 K attributed to most known clouds. In the first model—that of the continuously distributed gas—the dark matter density $\rho_{DM}(r)$ is simply given by the best fit PK profile used by Haller & Melia (1996), which is shown graphically in Figure 2. A lower limit to the size of the clouds in the second model is the Jeans radius R_J (Jeans 1902), below which the gas condensation will have collapsed and possibly formed stars. In terms of the cloud mass M_c and mean molecular weight μ, this limiting radius is given as

$$R_J \equiv \frac{3\mu\, m_H\, GM_c}{\pi^2\, kT}\ , \qquad (18)$$

where m_H is the proton mass. For simplicity, we shall adopt this value as the characteristic radius of all the (spherical) clouds in the system, and assume that they have uniform average density, given by

$$< \rho_c >= \frac{3\, M_c}{4\pi\, R_J^3}\ . \qquad (19)$$

Defining $n_c(r)$ to be the cloud number density as a function of radius, it is clear that in this case

$$\rho_{DM} = n_c(r)\, M_c\ . \qquad (20)$$

Numerically, for 10 $M_\odot$ clouds, $R_J \sim 2 \times 10^{-2}$ pc and $< \rho_c > \sim 3 \times 10^5\ M_\odot$ pc^{-3}. For these cloud characteristics, the volume filling factor in Draco would be about 2.8×10^{-8}, with an areal filling factor of roughly 1×10^{-3}. From an observational point of view, only about 0.1 % of Draco would therefore be obscured by all the clouds viewed as a whole, which would be consistent with the observed lack of extinction within this system. The cloud number density is about 9×10^{-2} pc^{-3} at the center of the dSph and falls off rapidly towards zero as the tidal radius is approached. Thus, a typical spacing of the clouds in the center of Draco is approximately 2 pc.

As discussed in § 2 above, the observed average dust grain size in many Galactic locations appears to be about 0.5 μm, but because the important dust destruction mechanisms that limit the grain size are presumably not functioning in dSphs, we consider values as high as $\approx$ 48 μm in our calculations. We also assume that the cosmic ray intensity in Draco is much lower than in the Galactic plane, and we take the FUV flux to be about 1.6 ($= S_{flux}$) times as large as Habing's (1968) value on the basis of our discussion in § 4 above. Finally, the gas turbulent velocity dispersion is taken to be the usual $\sim$ 1 km s^{-1} typically seen in most interstellar clouds in the solar neighborhood for the clumpy case, and equal to the total velocity dispersion in Figure 3 for the continuous case.

The calculational procedure calls for the simultaneous solution of 32 non-linear differential equations to determine the equilibrium density of each species at discrete steps into the cloud(s). Using the interaction network developed in § 5 above, all of these equations may be written in the generic form (for each species i)

$$\frac{dn_i}{dt} = \sum_{j,k} k_{ijk}^{gp+}\, n_j\, n_k + \sum_j k_{ij}^{pp+}\, n_j + \sum_j k_{ij}^{cr+}\, n_j - n_i \sum_j k_{ij}^{gp-}\, n_j$$

$$-n_i \sum_j k_j^{pp-} - n_i \sum_j k_j^{cr-}\ , \qquad (21)$$

where superscripts "+" and "–" stand for creation and annihilation processes, respectively, gp is for gas processes, pp is for photo-processes, and cr stands for cosmic ray. In equilibrium, $dn_i/dt = 0$, and the equations may be solved simultaneously using the

Newton-Raphson method. Starting with the full (unattenuated) FUV flux at the cloud surface, we integrate inwards, taking into account the gradual extinction of the radiation, until the densities of the various species reach their asymptotic (i.e., as $r \rightarrow 0$) values. This steady state is brought on by the attenuation of the incoming radiation by the dust and H_2 to the point where the reaction rates at smaller radii are affected primarily by the internal energy of the clouds. In every case, the radiation is attenuated significantly and the species reach their asymptotic values within a small fractional percentage of the cloud's radius near the surface, justifying a plane parallel treatment of the radiative transfer in this region (see below).

In Figure 10, we show the equilibrium distribution of the dominant species (H, H_2, and H_2^*) as a function of the radius (in pc) within Draco, for the case of a continuously distributed gas. The FUV flux induces rapid changes near the dSph's surface until the rapidly increasing visual extinction into the cloud and the H_2 self-shielding quenches the radiation field and the gas converts almost entirely to H_2. The assumed grain size for this simulation is 48 μm. This distribution has two major difficulties: (1) the corresponding total atomic hydrogen content is $M_H \approx 10^5\ M_\odot$, and (2) the visual extinction through the galaxy would be $A_v \approx 1.7 \times 10^5$. Both of these are inconsistent with the observations, which indicate that Draco is effectively transparent and that it contains at most $\sim 68\ M_\odot$ of atomic hydrogen (see § 2).

By comparison, these difficulties are not present when the gas is clumpy, say in the form of 10 $M_\odot$ clouds. The equilibrium profiles for this case are shown in Figures 11a), b), and c) assuming the same FUV flux and dust content as those above. For a hydrogen column density N_H to the center of each cloud (though concentrated primarily near its surface), the total hydrogen content of Draco may be estimated according to the equation

$$M_H \approx \frac{M_{DM}}{M_c}\, 4\pi\, R_c^2\, N_H\, m_H\ , \tag{22}$$

where M_{DM} is the total mass of dark matter in this system, and M_c and R_c are the individual cloud mass and radius, respectively. For this simulation, we find that $N_H \approx$

9.7×10^{17} cm^{-2}, for which $M_H \approx 67\ M_\odot$. We note that the corresponding visual extinction through each cloud is $A_v \approx 1.1 \times 10^7$. However, as noted earlier, the areal filling factor for this case is only $\sim 0.1\%$ so that typical lines-of-sight through this system would presumably not encounter any significant extinction.

Reducing the dust grain size drives the equilibrium away from H_2 towards H since the attenuation of the external FUV radiation is then not as effective. So, for example, if we reduce r_g to $\sim 0.7\ \mu$m, Draco would then need about 500 times more dust in order not violate the 21 cm limit on H. We will discuss the various observational implications of these results in the next section.

7. Observational Implications

On the basis of the 21 cm data, it would appear that the dark matter in Draco could be mostly H_2, but only if it is in the form of $\sim 10 - 100\ M_\odot$ clouds and if the dust grains are typically at least ~ 90 times larger than those in the Galaxy. This might be consistent with the fact that the dominant size-dependent dust destroying mechanisms in our galaxy are absent in typical dSphs. Interestingly, the absence of dynamical processes (such as supernova explosions) that would normally induce massive star formation (which is non-existent in Draco) may also account for this difference in the dust structure. A continuously distributed gas is ruled out by the lack of any observed extinction in this system, which would, however, be consistent with the very low areal covering fraction ($\sim 0.1 - 1\%$) if the dust and gas were concentrated in clouds.

We may estimate a gross upper limit to the FIR flux produced by the dust by simply taking the intercepted UV radiation and assuming that it is completely reprocessed into this longer wavelength band. Thus, using a FUV flux of $\approx 5.3 \times 10^{-3}$ ergs cm^{-2} s^{-1} at Draco, the $\approx 10^6$ 10 $M_\odot$ clouds, each with a radius of $\approx 2 \times 10^{-2}$ pc, would intercept a total radiative power of 6×10^{37} ergs s^{-1}. At earth, a conservative upper limit to the FIR flux from dust would therefore be 1×10^{-10} ergs cm^{-2} s^{-1}, or approximately 0.3 Jy if it is all emitted near 10 μm. By comparison, the IRAS sensitivity at this wavelength

is ≈ 0.07 Jy (Fazio & Eisenhardt 1990). In reality, only a small fraction of the FUV flux can actually be reprocessed in this fashion, and so this number must be a very generous estimate. That is, observations with current instruments probably would not be able to detect this dust emission. SIRTF is projected to have a sensitivity of 6×10^{-6} Jy at 10 μm, but it too may not be able to detect this dust since its field of view is too small to observe more than a small fraction of the entire dSph.

The situation also does not appear to be promising when it comes to the H_2 emission within the J and K bands. In Figures 12a) and b) we show the expected H_2^* spectrum (K and J infrared bands, respectively) integrated over the entire volume in Draco, as seen at earth. These are based on the 236 strongest infrared emission lines of excited H_2 ranging in wavelength from 12 μm to 0.85 μm, as described by Black & VanDishoeck (1987). NICMOS on HST will be an assembly of 3 cameras, with various fields of view (FOV) and a range of filters (Thompson 1996). Our predicted line flux in the K band is typically $\sim 2 \times 10^{-21}$ ergs cm^{-2} s^{-1}, but with its actual FOV, Camera 2 (which is sensitive in the wavelength range $1.75 - 2.35$ μm) will be able to sample about 10^{-5} of Draco's volume with a pointed integration at its center. At this level, it would not be able to detect the clouds in any reasonable integration time.

In the J band, the expected line flux for the most prominent components is typically $\sim 9 \times 10^{-22}$ ergs cm^{-2} s^{-1}, and using the same assumptions for Camera 1 (which is sensitive in the wavelength range $1.0 - 1.8$ μm, has a slightly smaller FOV and should be able to sample roughly 8×10^{-6} of Draco's volume), none of these lines will be easily detectable. The prospects for detection of these J band lines are similar with Camera 3, even though it has a larger FOV.

8. Concluding Remarks

Interestingly, similar considerations as the ones we have described here were sketched out earlier by Jura (1977) for elliptical galaxies. He speculated that because the UV radiation in these systems is low, the interstellar clouds in ellipticals may be cold and

largely H_2. As a result, the very low mass clouds ($M \lesssim 10\ M_\odot$) may collapse to create stars, and only late type stars may form. The conditions we have explored for the dSph galaxies are not unlike these. Our conclusions would seem to indicate that star formation within systems such as Draco may be largely dependent on which clouds can collapse without substantial external influence. If supernova-induced shocks or large-scale density waves are instrumental in producing large mass condensations that lead to the formation of early type stars, the general absence of these in dSphs may be consistent with the fact most of the clouds in these galaxies may not have undergone this type of dynamically-induced collapse. As a result, most of the mass (perhaps as much as 99%) may still be in the form of primordial H_2 clouds and only late type stars formed from the few lower mass clouds that crossed below the Jeans criterion.

Finally, we check to see whether such a "cluster" of H_2 clouds could in fact have avoided core collapse over a Hubble time t_H. Since the clouds presumably dominate the mass of the system, we may use the simple estimate (Binney & Tremaine 1987) of the core collapse time scale $t_{cc} \approx 12 - 19\ t_{rh}$ for a single mass component in terms of the median relaxation time

$$t_{rh} \equiv \frac{0.14 N_c}{\ln(0.4 N_c)} \sqrt{\frac{r_h^3}{G M_{DM}}}\ , \tag{23}$$

where N_c is the number of clouds, r_h is the system's median radius and M_{DM} is the total mass of dark matter. For Draco, $t_{cc} \sim 1 \times 10^{12} - 1.5 \times 10^{12}$ years, much longer than t_H.

This research was supported by NSF (PHY 88-57218) and NASA (NAGW-2822). We are very grateful to R. Kurucz for sending us his calculated stellar spectra, and to E. Olszewski for informative discussions and for providing the velocity data for Draco.

References

Aaronson, M. & Olszewski, E.W. 1987, in *Dark Matter in the Universe*, ed. J. Kormendy & G.R. Knapp (Reidel: Dordrecht), p. 153.

Allen, C. W. 1973, Astrophysical Quantities, 3rd ed. (London: Athlone Press).

Bahcall, J. N. 1986, Ann. Rev. Astron. Astrophys, 24, 577.

Bahcall, J. N. & Maoz D. 1993, Ap. J. Supp., 88, 53.

Bahcall, J. N. & Soneira R. M. 1981, Ap. J., 246, 122.

Bahcall, J.N. & Tremaine, S. 1981, Ap. J., 244, 805. (BaT)

Binney, J. & Tremaine, S. 1987, Galactic Dynamics, Princeton University Press.

Black, J. H. & Dalgarno, A. 1977, Ap. J. Supp., 34, 405.

Black, J. H. & VanDishoeck, E. F. 1987, Ap. J., 322, 412.

Da Costa, G.S. 1992, in *Stellar Populations of Galaxies*, ed. B. Barbuy & A. Renzini (Kluwer: Dordrecht).

Draine, B. T. 1978, Ap. J. Supp., 36, 595.

Draine, B. T. & Salpeter, E. E. 1979, Ap. J., 231, 438.

Elmgreen, B.G. 1993, Ap. J., 411, 170.

Fazio, G. G. & Eisenhardt, P. 1990, in Observatories in Earth Orbit and Beyond, Ed. Y. Kondo (Dordrecht: Kluwer), p. 193.

Gerhard, O.E. & Spergel, D.N. 1992, Ap. J. Letters, 389, L9.

Gould, R. J. & Harwit, M. 1963, Ap. J. 137, 694.

Habing, H. J. 1968 Bull. Astr. Inst. Netherlands, 19, 421.

Haller, J.W. & Melia, F. 1996, Ap. J., 446, in press.

Heisler, J., Tremaine, S., & Bahcall, J.N. 1985, Ap. J., 298, 8. (HTB)

Hodge, P. W. 1971, Ann. Rev. Astron. Astrophys, 9, 35.

Jeans, J. 1902, Phil. Trans. Roy. Soc. London, A 199, 1.

Jura, M. 1975, Ap. J., 197, 575.

Jura, M. 1977, Ap. J., 212, 634.

King, I.R. 1966, A.J., 71(1), 64.

Knapp, G.R., Kerr, F.J. & Bowers, P.F. 1978, A.J., **83**, 360.

Kurucz, R. L., 1993, Kurucz CD-ROM No 13.

Martin, P. G. 1978, Cosmic Dust, Its Impact On Astronomy (Clarendon Press: Oxford).

Martin, C., Hurwitz, M. & Bowyer, S. 1990, Ap. J., 354, 220.

Martin, C., Hurwitz, M. & Bowyer, S. 1991, Ap. J., 379, 549.

Mateo, M., Olszewski, E.W., Welch, D.L., Fischer, P. & Kunkel, W. 1991, A.J., **102**, 914.

Mihalas, D. and Binney, J. 1981, Galactic Astronomy-Structure and Kinematics, (San Francisco: W. H. Freeman and Company).

Mould, J., et al. 1990, *Ap. J. (Letters)*, **362**, L55.

Olszewski E. 1994, private communication.

Paltoglou, G. & Freeman, K.C. 1987, in *Structure and Dynamics of Elliptical Galaxies*, ed. T. de Zeeuw, (Reidel: Dordrecht), p. 447.

Paresce, F. & Jakobsen, P. 1980, Nature 288, 119.
Prasad, S. S. & Huntress, W. T. Jr. 1985, Ap. J. Supp., 43, 1.
Pryor, C. & Kormendy, J. 1990, A.J., 100, 127. (PK).
Roberge W. G. 1981, Topics in the Physics of Interstellar Clouds, Ph.D. Dissertation, (Ann Arbor: UMI).
Rogerson, J.B. et al. 1973, Ap. J. Letters, 181, L97.
Savage , B. D. & Mathis J. S. 1979, Ann. Rev. Astr. Ap., 17, 73.
Scott, E.H. & Rose, W.K. 1975, Ap. J., 197, 147.
Shull, J. M. & Becwith, S. 1982, Ann. Rev. Astron. Astrophys., 20, 163.
Spitzer, L. 1978, Physical Processes in the Interstellar Medium (New York: John Wiley & Sons).
Sternberg, A. & Dalgarno, A. 1989, Ap. J., 338, 197.
Stetson P. B. 1980, A. J., 85, 387.
Strobel & Lake 1994, Ap. J. Lett., 424, L83.
Thompson, R. 1996, private communication.
Tielens, A. G. G. M. & Hollenbach, D. 1985, Ap. J., 291, 722.
VanDishoeck, E. F. & Black, J. H. 1986, Ap. J. Supp., 62, 109.
Young, P.J. 1980, Ap. J., 242, 1232.
Zinn, R. 1978, Ap. J., 225, 790.

TABLE 1A

Luminosity Class V - VII (main sequence, sub dwarfs and white dwarfs)

model #	Spectral Type	Teff	log(g)	log(Rs/R⊙)	[M/H]*	Kurucz model #	Kurucz Teff	Kurucz log(g)
D1	O5(O5-O9)	47000	4	1.25	0	408	47500	5
D2	B0(B0-B4)	30500	4	0.87	0	387	31000	4
D3	B5(B5-B9)	15000	4.1	0.58	0	308	15000	4
D4	A0(A0-A4)	9500	4.1	0.4	0	244	9500	4
D5	A5(A5-A9)	8300	4.2	0.24	0	214	8500	4
D6	F0(F0-F4)	7300	4.3	0.13	0	179	7500	4
D7	F5(F5-F9)	6600	4.3	0.08	0	149	6750	4
D8	G0(G0-G4)	5900	4.4	0.02	0	119	6000	4
D9	G5(G5-G9)	5600	4.5	-0.03	0	109	5750	4.5
D10	K0(K0-K4)	5100	4.5	-0.07	0	87	5250	4.5
D11	K5(K5-K9)	4200	4.5	-0.13	0	43	4250	4.5
D12	M0(M0-M4)	3700	4.6	-0.2	0	21	3750	4.5
D13	M5(M5-M9)	3000	4.8	-0.5	0	11	3500	5

Stellar parameters are from Mihalas & Binney (1981), unless otherwise stated

*Metallicity ([M/H]=log[n(Fe)/n(H)] - log[n(Fe)/n(H)]⊙)

TABLE 1B

Luminosity Class III - IV (giants and subgiants)								
model #	Spectral Type	Teff	log(g)	log(Rs/R⊙)	[M/H]*	Kurucz model #	Kurucz Teff	Kurucz log(g)
G1	O5(O5-O9)	~44500	~3.9	~1.3	0	407	45000	5
G2	B0(B0-B4)	~28000	3.8	1.2	0	375	28000	4
G3	B5(B5-B9)	~14250	3.7	1	0	308	15000	4
G4	A0(A0-A4)	~8750	3.7	0.8	0	222	8750	4
G5	A5(A5-A9)	~7550	3.6	~0.775	0	187	7750	3.5
G6	F0(F0-F4)	~6850	3.5	~0.725	0	158	7000	3.5
G7	F5(F5-F9)	~6150	3.5	0.6	0	128	6250	3.5
G8	G0(G0-G4)	5400	3.3	0.8	0	96	5500	3.5
G9	G5(G5-G9)	4800	3	1	0	73	5000	3
G10	K0(K0-K4)	4400	2.6	1.2	0	50	4500	2.5
G11	K5(K5-K9)	3600	1.9	1.4	0	16	3750	2
G12	M0(M0-M4)	3300	1.4	1.88**	0	4	3500	1.5
G13	M5(M5-M9)	2700	~1	2.01**	0	3	3500	1

Stellar parameters are from Mihalas & Binney (1981), unless otherwise stated

*Metallicity ([M/H]=log[n(Fe)/n(H)] - log[n(Fe)/n(H)]⊙)

~These values are extrapolated from the available data.

**From Allen (1973).

TABLE 1C

Luminosity Class I - II (super giants and bright giants)								
model #	Spectral Type	Teff	log(g)	log(Rs/R⊙)	[M/H]*	Kurucz model #	Kurucz Teff	Kurucz log(g)
S1	O5(O5-O9)	~42000	3.4**	~1.35	0	406	42500	5
S2	B0(B0-B4)	25500	3.1	1.3	0	365	26000	3
S3	B5(B5-B9)	13500	2.8	1.5	0	300	14000	3
S4	A0(A0-A4)	~8000	2.4	1.6	0	194	8000	2.5
S5	A5(A5-A9)	~6800	2.1	1.7	0	155	7000	2
S6	F0(F0-F4)	6400	1.9	1.8	0	135	6500	2
S7	F5(F5-F9)	~5700	1.7	1.9	0	104	5750	2
S8	G0(G0-G4)	5400	1.5	2	0	92	5500	1.5
S9	G5(G5-G9)	4700	1.3	2.1	0	59	4750	1.5
S10	K0(K0-K4)	4000	1	2.3	0	25	4000	1
S11	K5(K5-K9)	3400	0.6	2.6	0	2	3500	0.5
S12	M0(M0-M4)	2800	0.2	2.7	0	1	3500	0
S13	M5(M5-M9)	~2200	~0	~2.8	0	1	3500	0

Stellar parameters are from Mihalas & Binney (1981), unless otherwise stated

*Metallicity ([M/H]=log[n(Fe)/n(H)] - log[n(Fe)/n(H)]⊙)

~These values are extrapolated from the available data.

**From Allen (1973).

TABLE 2A

Luminosity Class V - VII (main sequence, sub dwarfs and white dwarfs)			
model #	Spectral Type	percentage	number of stars*
D1	O5(O5-O9)	0.000048935	4.89350E+04
D2	B0(B0-B4)	0.012532	1.25320E+07
D3	B5(B5-B9)	5.0004	5.00040E+09
D4	A0(A0-A4)	5.4024	5.40240E+09
D5	A5(A5-A9)	2.3153	2.31530E+09
D6	F0(F0-F4)	3.4817	3.48170E+09
D7	F5(F5-F9)	3.4817	3.48170E+09
D8	G0(G0-G4)	4.444	4.44400E+09
D9	G5(G5-G9)	4.444	4.44400E+09
D10	K0(K0-K4)	4.8373	4.83730E+09
D11	K5(K5-K9)	4.8373	4.83730E+09
D12	M0(M0-M4)	30.376	3.03760E+10
D13	M5(M5-M9)	30.376	3.03760E+10

*Based on a total of 1E+11 stars in the galaxy.

TABLE 2B

Luminosity Class III - IV (giants and subgiants)			
model #	Spectral Type	percentage	number of stars*
G1	O5(O5-O9)	0.000000434	4.34000E+02
G2	B0(B0-B4)	2.5917E-06	2.59170E+03
G3	B5(B5-B9)	0.0010341	1.03410E+06
G4	A0(A0-A4)	0.016879	1.68790E+07
G5	A5(A5-A9)	0.0072339	7.23390E+06
G6	F0(F0-F4)	0.10455	1.04550E+08
G7	F5(F5-F9)	0.10455	1.04550E+08
G8	G0(G0-G4)	0.12361	1.23610E+08
G9	G5(G5-G9)	0.12261	1.22610E+08
G10	K0(K0-K4)	0.23635	2.36350E+08
G11	K5(K5-K9)	0.23635	2.36350E+08
G12	M0(M0-M4)	0.01742	1.74200E+07
G13	M5(M5-M9)	0.01742	1.74200E+07

*Based on a total of 1E+11 stars in the galaxy.

TABLE 2C

Luminosity Class I - II (super giants and bright giants)			
model #	Spectral Type	percentage	number of stars*
S1	O5(O5-O9)	0.00000027	2.70000E+02
S2	B0(B0-B4)	1.2565E-06	1.25650E+03
S3	B5(B5-B9)	3.7695E-06	3.76950E+03
S4	A0(A0-A4)	0.000073819	7.38190E+04
S5	A5(A5-A9)	0.000031637	3.16370E+04
S6	F0(F0-F4)	0.00022851	2.28510E+05
S7	F5(F5-F9)	0.00022851	2.28510E+05
S8	G0(G0-G4)	0.00032297	3.22970E+05
S9	G5(G5-G9)	0.00032297	3.22970E+05
S10	K0(K0-K4)	0.00056577	5.65770E+05
S11	K5(K5-K9)	0.00056577	5.65770E+05
S12	M0(M0-M4)	0.0003636	3.63600E+05
S13	M5(M5-M9)	0.0003636	3.63600E+05

*Based on a total of 1E+11 stars in the galaxy.

TABLE 3A

GAS PHASE REACTIONS

Number	Reaction	A	α	β
PI15	$He^+ + H_2 \rightarrow H^+ + H + He$	1.5(-13)	0.00	0.00
PI49	$H_2^+ + H \rightarrow H^+ + H_2$	1.0(-10)	0.00	0.00
PI43	$O^+ + H_2 \rightarrow OH^+ + H$	1.6(-09)	0.00	0.00
PI42	$O^+ + H \rightarrow O + H^+$	7.0(-10)	0.00	0.00
PI13	$He^+ + H \rightarrow He + H^+ + h\nu$	1.9(-15)	0.00	0.00
PI12	$H^+ + H_2O \rightarrow H + H_2O^+$	8.2(-09)	0.00	0.00
PI1	$H^+ + O \rightarrow H + O^+$	7.0(-10)	0.00	232.0
PI32*	$C^+ + OH \rightarrow CO + H^+$	7.7(-10)	0.00	0.00
PI32	$C^+ + OH \rightarrow CO^+ + H$	7.7(-10)	0.00	0.00
PI50	$H_2^+ + H_2 \rightarrow H_3^+ + H$	2.1(-09)	0.00	0.00
PI19	$He^+ + CO \rightarrow He + C^+ + O$	1.6(-09)	0.00	0.00
PI65	$H_3^+ O \rightarrow OH^+ + H_2$	8.0(-10)	0.00	0.00
PI59	$OH^+ + H_2 \rightarrow H_2O^+ + H$	1.1(-09)	0.00	0.00
PI79	$H_2O^+ + H_2 \rightarrow H_3O^+ + H$	6.1(-10)	0.00	0.00
PI38	$C^+ + H_2O \rightarrow HCO^+ + H$	2.7(-09)	0.00	0.00
PI61	$CO^+ + H_2 \rightarrow HCO^+ + H$	2.0(-09)	0.00	0.00
PI69	$H_3^+ + CO \rightarrow HCO^+ + H_2$	1.7(-09)	0.00	0.00
PI27	$C^+ + O_2 \rightarrow CO^+ + O$	7.5(-10)	0.00	0.00
PI28	$C^+ + O_2 \rightarrow CO + O^+$	4.1(-10)	0.00	0.00
PI16	$He^+ + O_2 \rightarrow He + O + O^+$	1.0(-09)	0.00	0.00
NR4	$O + OH \rightarrow O_2 + H$	3.0(-11)	-.36	0.00

Rate coefficients are from Prasad & Huntress (1980), unless otherwise stated.
Number notation: 1.0(-10) = 1.0×10^{-10}
*From Roberge (1981).

TABLE 3B

ELECTRON RECOMBINATION REACTIONS

Number	Reaction	A	α	β
AI1	$H^+ + e^- \rightarrow H + h\nu$	3.5(-12)	-.70	0.00
EI12	$H_3^+ + e^- \rightarrow H_2 + H$	1.1(-07)	-.50	0.00
EI13	$H_3^+ + e^- \rightarrow H + H + H$	1.1(-07)	-.50	0.00
AI5	$O^+ + e^- \rightarrow O + h\nu$	3.4(-12)	-.63	0.00
EI7	$OH^+ + e^- \rightarrow O + H$	2.0(-07)	-.50	0.00
EI18	$H_2O^+ + e^- \rightarrow OH + H$	2.0(-07)	-.50	0.00
EI38	$H_3O^+ + e^- \rightarrow OH + H + H$	6.5(-07)	-.50	0.00
EI37	$H_3O^+ + e^- \rightarrow H_2O + H$	6.5(-07)	-.50	0.00
AI3	$C^+ + e^- \rightarrow C + h\nu$	4.4(-12)	-.61	0.00
AI2	$He^+ + e^- \rightarrow He + h\nu$	4.5(-12)	-.67	0.00
AI4	$N^+ + e^- \rightarrow N + h\nu$	3.8(-12)	-.62	0.00
AI9	$Mg^+ + e^- \rightarrow Mg + h\nu$	2.8(-12)	-.86	0.00
AI6	$Si^+ + e^- \rightarrow Si + h\nu$	4.9(-12)	-.60	0.00
AI7	$S^+ + e^- \rightarrow S + h\nu$	3.9(-12)	-.63	0.00
AI8	$Fe^+ + e^- \rightarrow Fe + h\nu$	3.7(-11)	-.65	0.00
EI8	$CO^+ + e^- \rightarrow C + O$	1.8(-07)	-.50	0.00
EI20	$HCO^+ + e^- \rightarrow H + CO$	2.0(-07)	-.75	0.00

Rate coefficients are from Prasad & Huntress (1980), unless otherwise stated.
Number notation: 1.0(-10) = 1.0×10^{-10}

TABLE 3C

COSMIC RAY REACTIONS

Number	Reaction	A	α	β
CR1	$H + cr \rightarrow H^+ + e^-$	4.6(-01)	0.00	0.00
CR2	$He + cr \rightarrow He^+ + e^-$	5.0(-01)	0.00	0.00
CR7	$H_2 + cr \rightarrow H_2^+ + e^-$	9.3(-01)	0.00	0.00
CR6	$H_2 + cr \rightarrow H + H^+ + e^-$	2.2(-02)	0.00	0.00
CR8	$H_2 + cr \rightarrow H + H$	1.0(-01)	0.00	0.00
CR3	$C + cr \rightarrow C^+ + e^-$	1.8(-00)	0.00	0.00
CR5	$O + cr \rightarrow O^+ + e^-$	2.8(-00)	0.00	0.00
CR10	$CO + cr \rightarrow CO^+ + e^-$	3.0(-00)	0.00	0.00
CR4	$N + cr \rightarrow N^+ + e^-$	2.1(-00)	0.00	0.00

Rate coefficients are from Prasad & Huntress (1980), unless otherwise stated.
Number notation: 1.0(-10) = 1.0×10^{-10}

TABLE 3D

PHOTOIONIZATION AND DISSOCIATION REACTIONS

Number	Reaction	A	α	β
PP55	$H_2 + h\nu \rightarrow H + H$		(See text)	
PP15	$OH + h\nu \rightarrow O + H$	2.2(-10)	0.00	2.0
PP27	$H_2O + h\nu \rightarrow H_2O^+ + e^-$	2.1(-11)	0.00	3.1
PP26	$H_2O + h\nu \rightarrow OH + H$	5.1(-10)	0.00	1.8
PP1	$C + h\nu \rightarrow C^+ + e^-$	2.1(-10)	0.00	2.6
PP17	$CO + h\nu \rightarrow C + O$	1.4(-11)	0.00	3.2
PP5	$Mg + h\nu \rightarrow Mg^+ + e^-$	4.4(-11)	0.00	1.4
PP2	$Si + h\nu \rightarrow Si^+ + e^-$	1.2(-09)	0.00	1.6
PP3	$S + h\nu \rightarrow S^+ + e^-$	3.9(-10)	0.00	2.5
PP4	$Fe + h\nu \rightarrow Fe^+ + e^-$	1.0(-10)	0.00	2.3
PP9	$O_2 + h\nu \rightarrow O + O$	3.3(-10)	0.00	1.4

Rate coefficients are from Prasad & Huntress (1980), unless otherwise stated.
Number notation: 1.0(-10) = 1.0×10^{-10}

TABLE 3E

ROTATION-VIBRATIONALLY EXCITED HYDROGEN REACTIONS

Number	Reaction	A	α	β
H21	$H + H + Grain \rightarrow H_2^* + Grain$		(See text)	
MH14	$H_2 + h\nu \rightarrow H_2^*$		(See text)	
MH1	$H_2^* + h\nu \rightarrow H + H$		(See text)	
MH13	$H_2^* \rightarrow H_2 + h\nu$	2.0(-07)	0.00	0.00
MH2	$H_2^* + H \rightarrow H_2 + H$	1.9(-12)	.50	1.0(03)
MH3	$H_2^* + H_2 \rightarrow H_2 + H_2$		(See text)	
MH4	$H_2^* + H \rightarrow H + H + H$	9.8(-12)	.50	2.7(04)
MH5	$H_2^* + H_2 \rightarrow H_2 + H + H$	9.8(-12)	.50	2.7(04)
MH6	$H_2^* + H_2^* \rightarrow H + H + H_2$	9.8(-12)	.50	0.00
MH7	$H_2^* + O \rightarrow OH + H$	9.0(-12)	1.00	0.00
MH8	$H_2^* + OH \rightarrow H_2O + H$	3.6(-11)	0.00	0.00
MH9	$H_2^* + O_2 \rightarrow OH + OH$	1.0(-10)	0.00	0.00

Rate coefficients are from Tielens & Hollenbach (1980), unless otherwise stated.
Number notation: 1.0(-10) = 1.0×10^{-10}

FIGURE CAPTIONS

Fig. 1. – The aperture PME applied to stellar radial velocity data (•) from the dwarf spheroidal galaxy Draco (Olszewski 1994). The data points with an open circle (○) include an additional high velocity star in the aperture PME. The data points are not independent; at a given projected radius, each point contains all of the stars within that radius. The solid line shows the computed aperture PME curve corresponding to a King model fit to the central velocity dispersion and stellar surface density from Pryor & Kormendy (1990; PK) with M/L = 100. The dashed and dotted lines correspond to the allowed range in the central black hole mass, (1.5-2.0)$\times 10^7$ $M_\odot$, for a model proposed by Strobel & Lake (1994; SL). On the whole, the data are more consistent with the King model. (From Haller & Melia 1996)

Fig. 2. – Dark mass density distribution for the best fit PK model (see text and Fig. 1).

Fig. 3. – Velocity as a function of radius within Draco: total velocity dispersion (solid), tangential velocity dispersion (short dash), radial velocity dispersion (dotted), Keplerian circular velocity (long dash), and local escape velocity (dot-dash). The vertical dashed line corresponds to the core radius at 117 pc.

Fig. 4. – Schematic diagram illustrating the simple model we adopt for the Milky Way galaxy. The stars are assumed to lie uniformly in a thin disk (the 'stellar' disk) with a radius of 15 kpc, embedded within a uniform disk of dust with a thickness of 300 pc. Draco lies at a heliocentric distance of 67 kpc, with a galactic latitude of 35 degrees and a galactic longitude of 86 degrees.

Fig. 5. – The percentage of galactic stars within each spectral type: main sequence (solid), giants (dotted), supergiants (dashed).

Fig. 6. – The average interstellar attenuation curve of Savage & Mathis (1979). Here, R_λ is the ratio of the magnitude of attenuation A_λ to $E(B-V)$, as a function of wavelength.

Fig. 7. – The total FUV spectrum at Draco due to the contributions from all the stars in the Milky Way galaxy, taking into account the proper attenuation through the galactic plane.

Fig. 8. – Same as Figure 7, except now in units of photons cm^{-2} s^{-1} $\mathring{A}^{-1}$.

Fig. 9. – Same as Figure 7, except now also showing for comparison the theoretical spectrum calculated for the interstellar medium by Habing (1968) in the wavelength range $912 - 3000$ $\mathring{A}$ (long dashed curve), here multiplied by a factor of 1.6, and Draine's (1978) spectrum in the wavelength band $912 - 2000$ $\mathring{A}$, which is based on the compilation of observational and theoretical data (short dashed curve). Draine's spectrum is here multiplied

by a factor of 1.7. In both cases, the multiplicative factor accounts for the differences in geometry (distance and degree of attenuation) between their case and ours.

Fig. 10. – Equilibrium distribution of the dominant species (as labeled) as a function of the radius (in pc) within Draco, for the case of a continuously distributed gas. The rapid changes near the dSph's outer surface are due to the effects of the external FUV radiation field (mostly from the Milky Way galaxy). The vertical dashed line indicates the core radius at 117 pc.

Fig. 11. – Same as Fig. 10, but now for a 10 $M_{\odot}$ cloud as described in § 6 of the text. The three different parts of this figure pertain to the hydrogen-based species (a), the oxygen-based species (b), and the carbon-based species (c).

Fig. 12. – The predicted H_2 spectrum integrated over the entire volume of Draco for a) K band and b) J band.

Figure 1

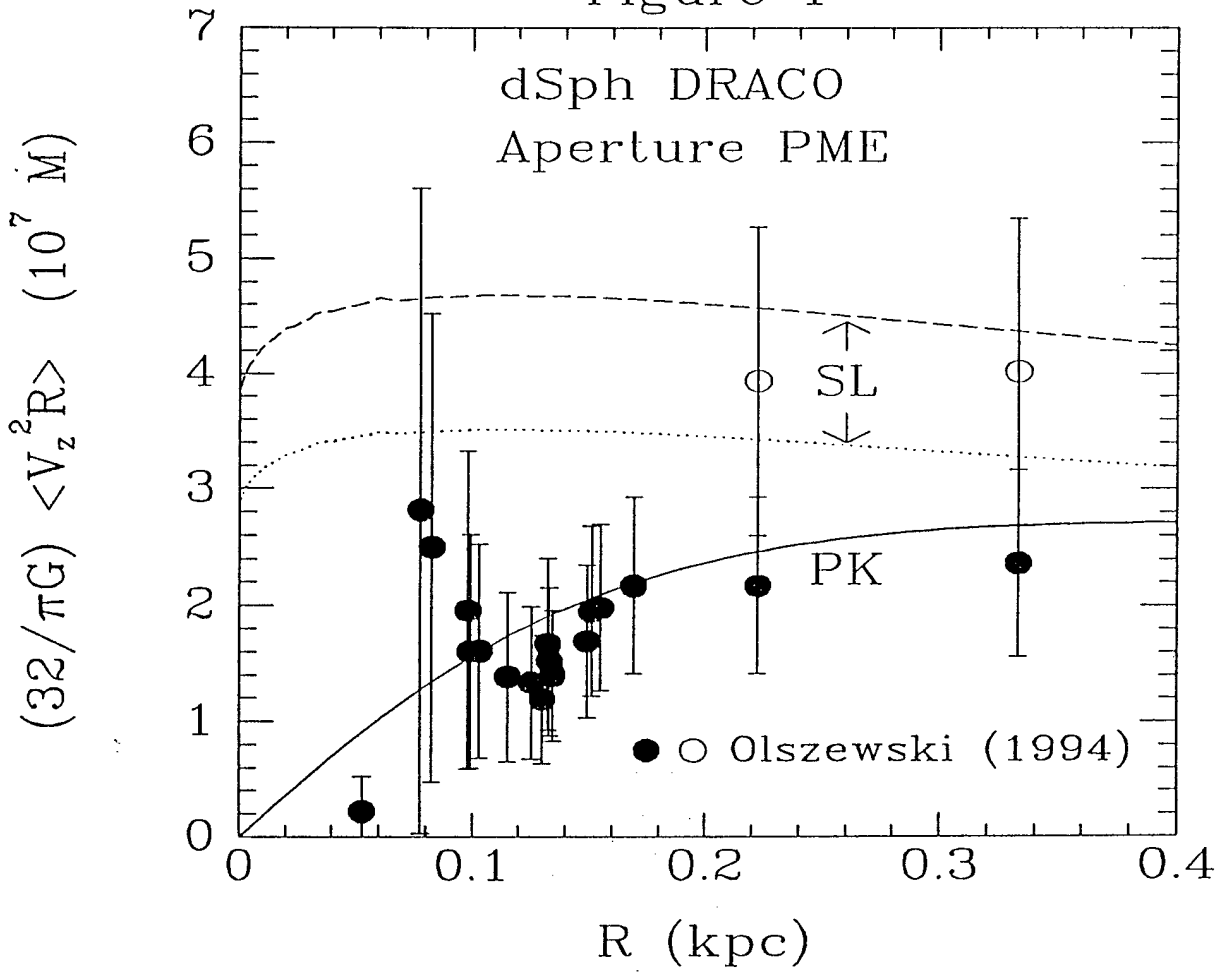
dSph DRACO
Aperture PME
SL
PK
Olszewski (1994)
$(32/\pi G)\ \langle V_z^2 R\rangle\ (10^7\ M_\odot)$
R (kpc)
0
1
2
3
4
5
6
7
0
0.1
0.2
0.3
0.4

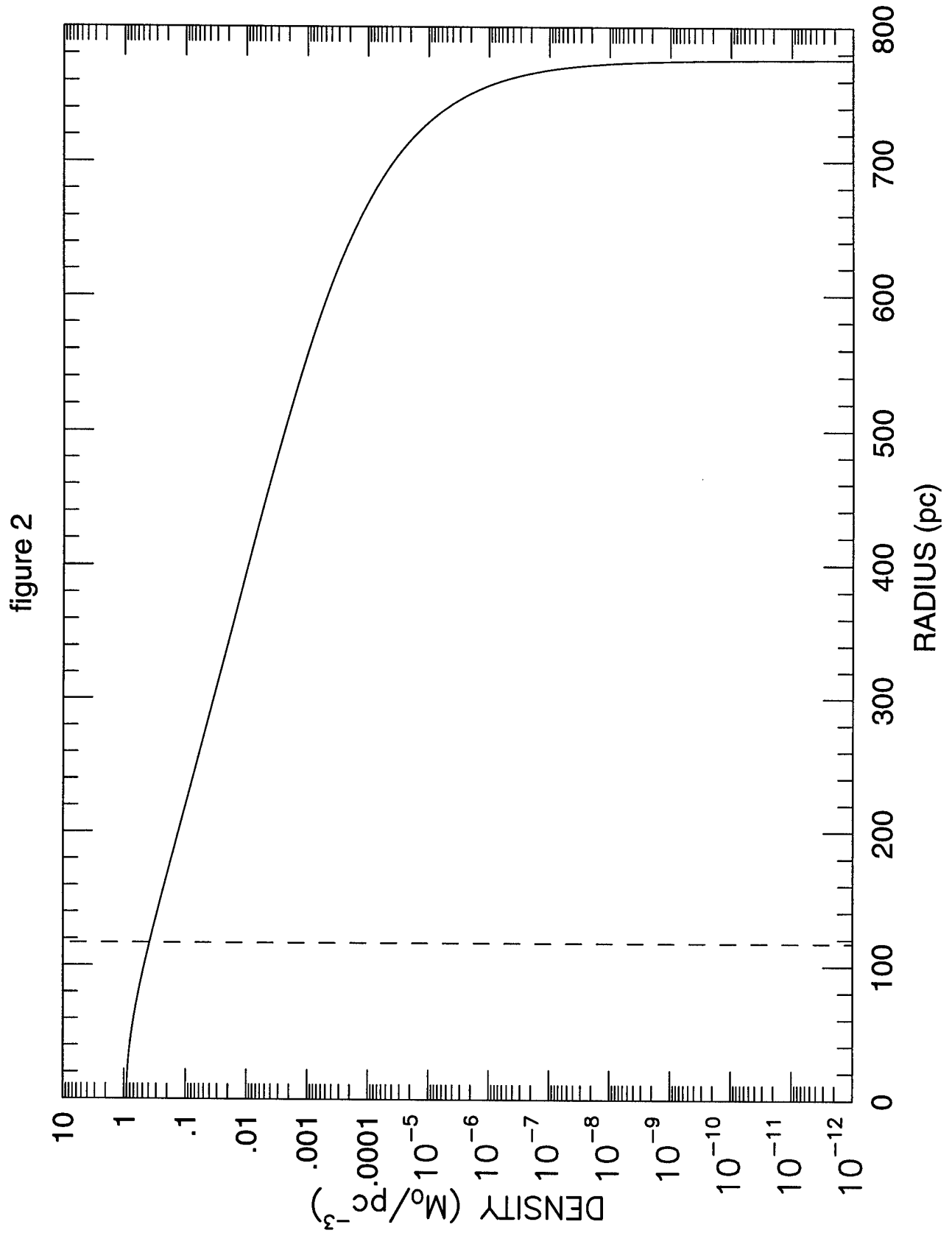
figure 2
DENSITY ($M_\odot/pc^{-3}$)
10
1
.1
.01
.001
.0001
10^{-5}
10^{-6}
10^{-7}
10^{-8}
10^{-9}
10^{-10}
10^{-11}
10^{-12}
0
100
200
300
400
500
600
700
800
RADIUS (pc)

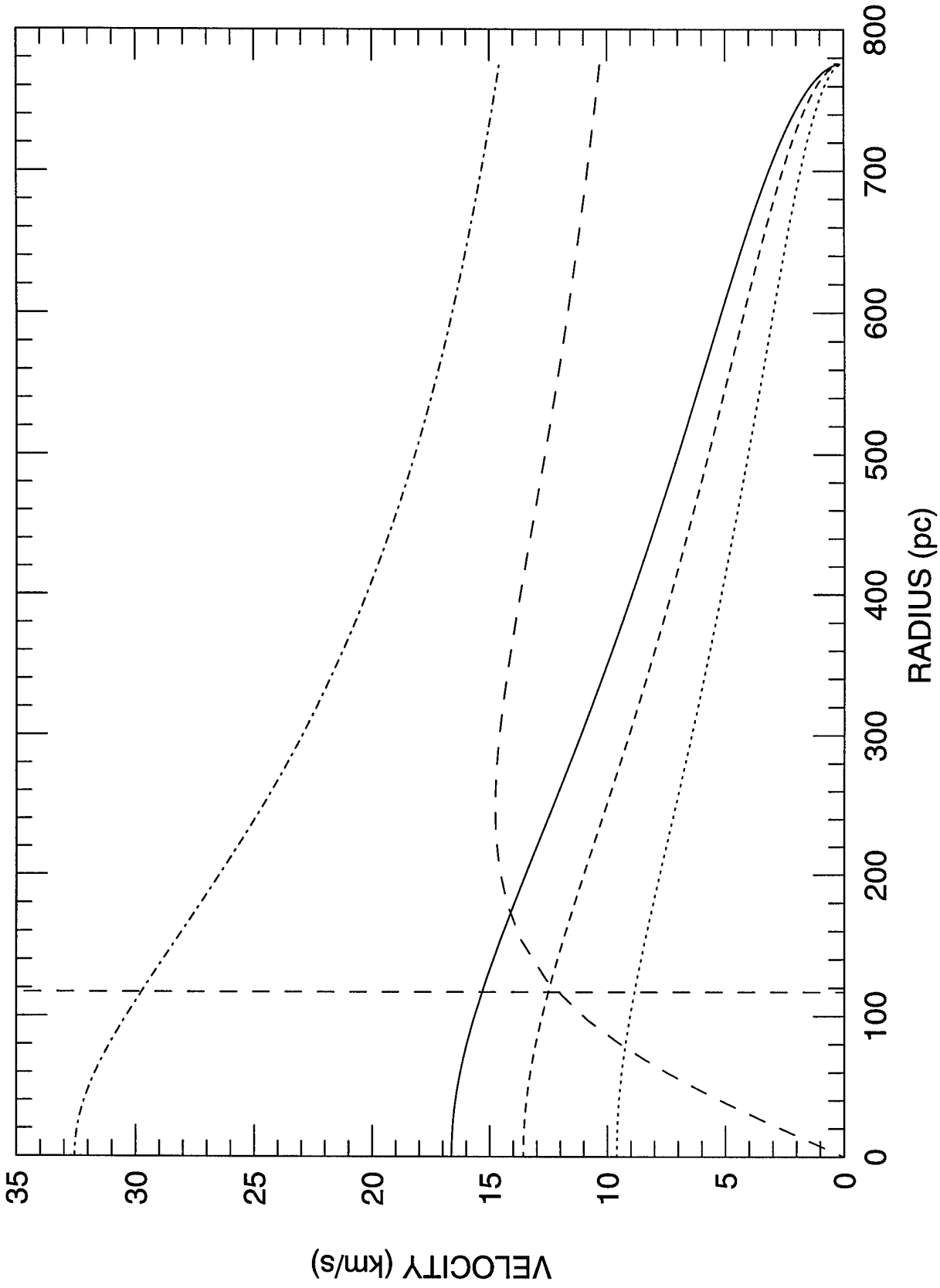
figure 3
VELOCITY (km/s)
RADIUS (pc)
0
5
10
15
20
25
30
35
0
100
200
300
400
500
600
700
800

figure 4

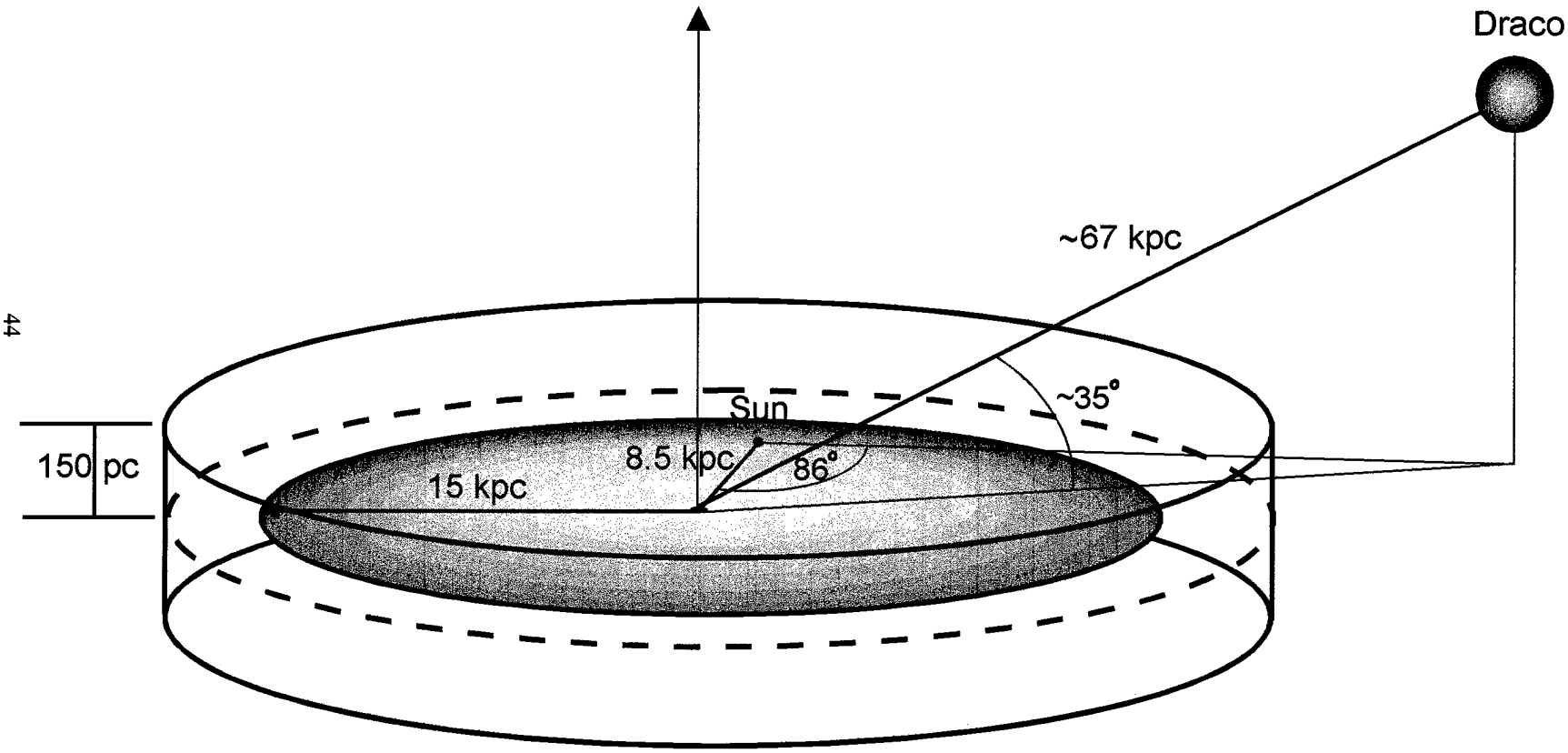

(not to scale)

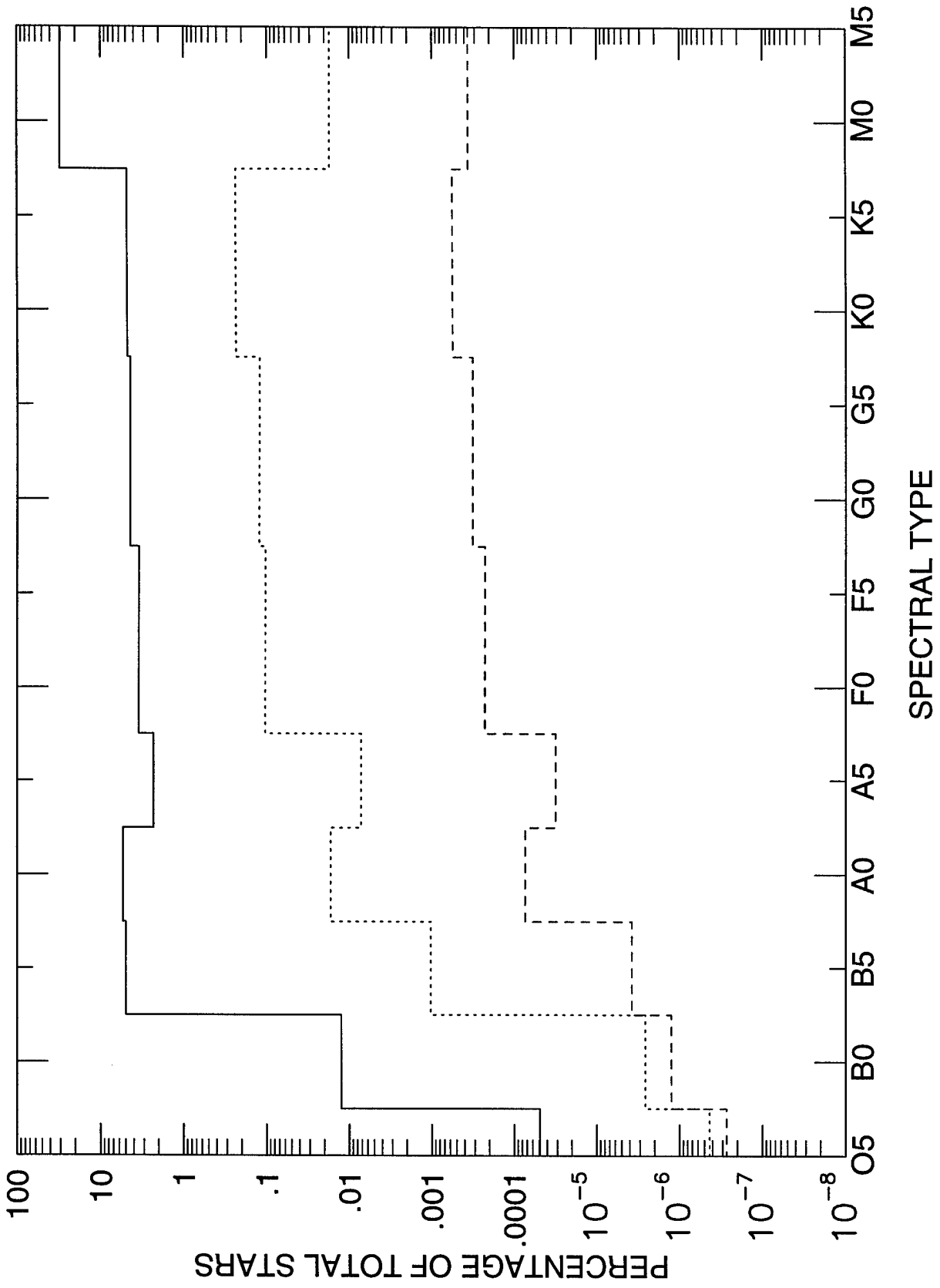
figure 5
PERCENTAGE OF TOTAL STARS
100
10
1
.1
.01
.001
.0001
10^{-5}
10^{-6}
10^{-7}
10^{-8}
O5
B0
B5
A0
A5
F0
F5
G0
G5
K0
K5
M0
M5
SPECTRAL TYPE

figure 6

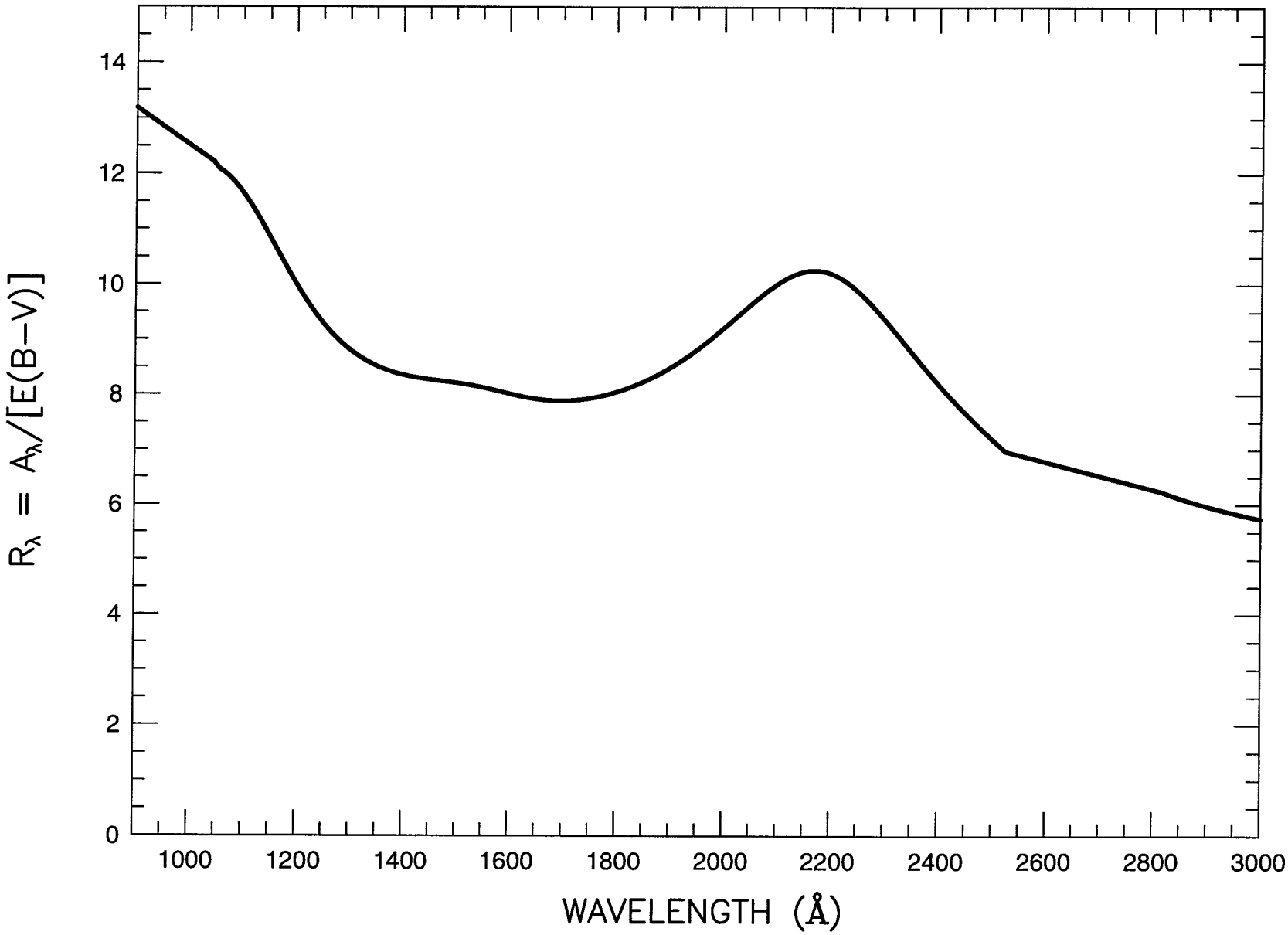
14
12
10
8
6
4
2
0
$R_\lambda = A_\lambda/[E(B-V)]$
1000
1200
1400
1600
1800
2000
2200
2400
2600
2800
3000
WAVELENGTH (Å)

figure 7

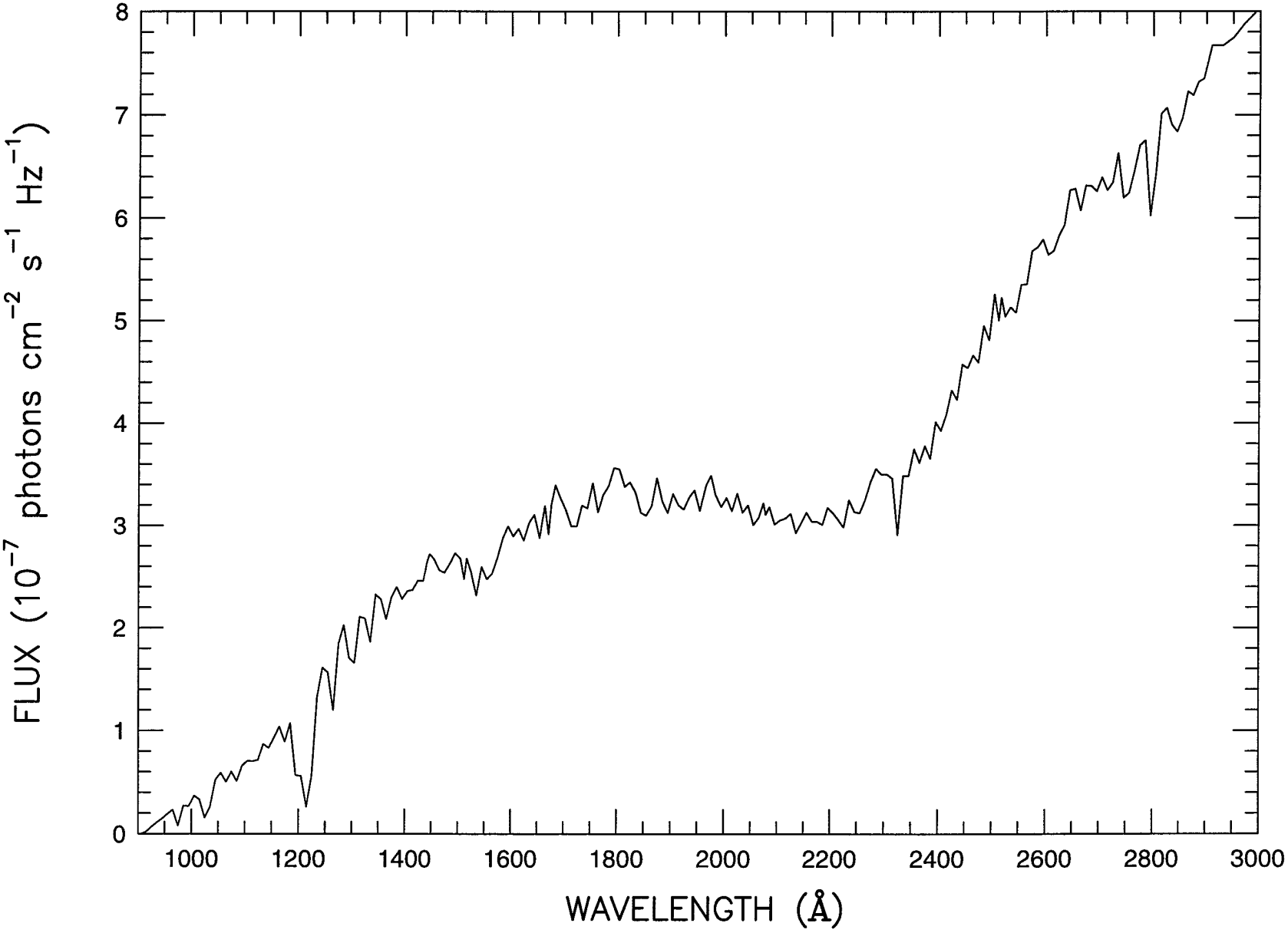
FLUX (10^{-7} photons cm^{-2} s^{-1} Hz^{-1})
0
1
2
3
4
5
6
7
8
1000
1200
1400
1600
1800
2000
2200
2400
2600
2800
3000
WAVELENGTH (Å)

figure 8

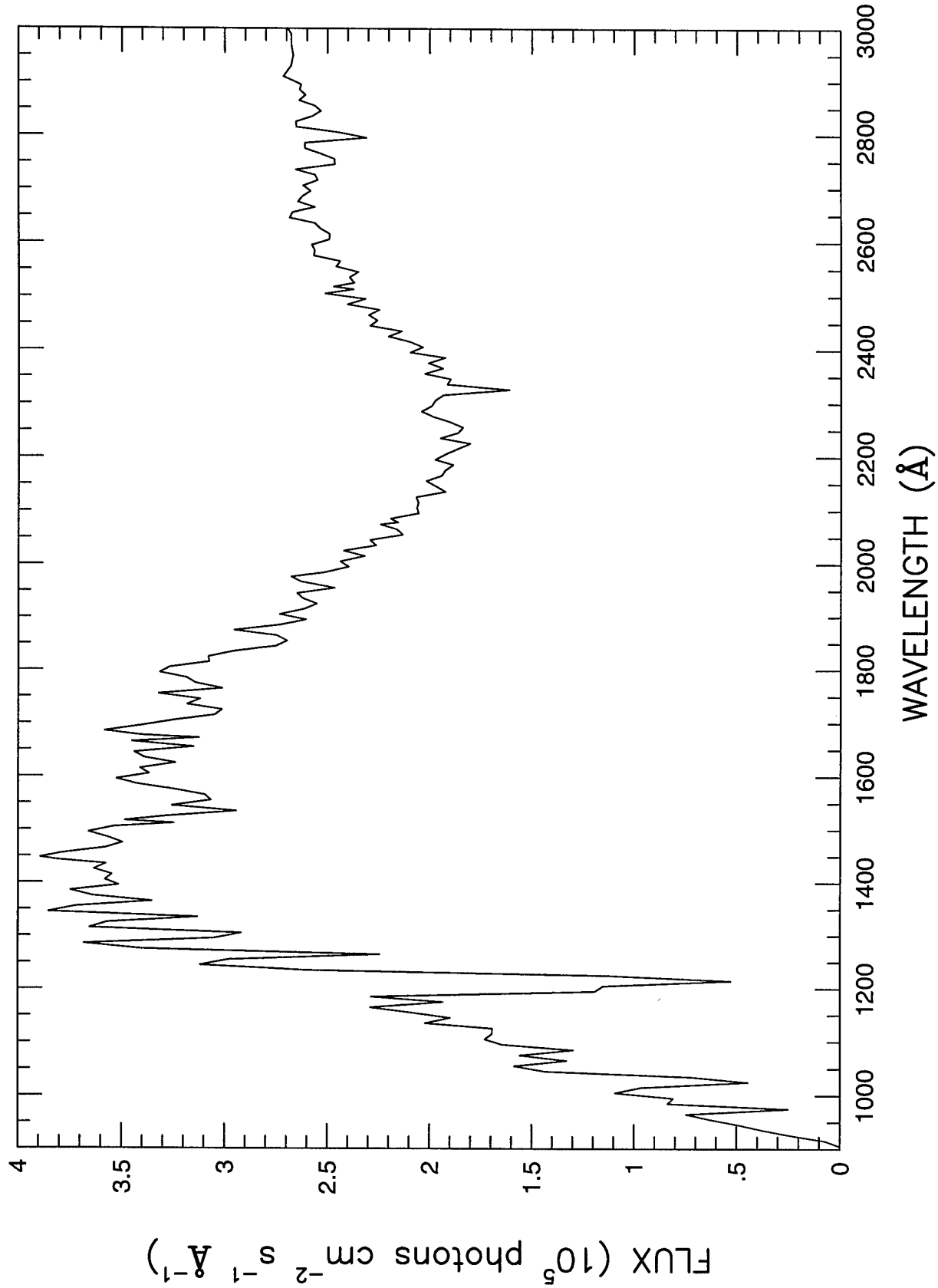
FLUX (10^5 photons cm^{-2} s^{-1} $Å^{-1}$)
0
.5
1
1.5
2
2.5
3
3.5
4
1000
1200
1400
1600
1800
2000
2200
2400
2600
2800
3000
WAVELENGTH (Å)

figure 9

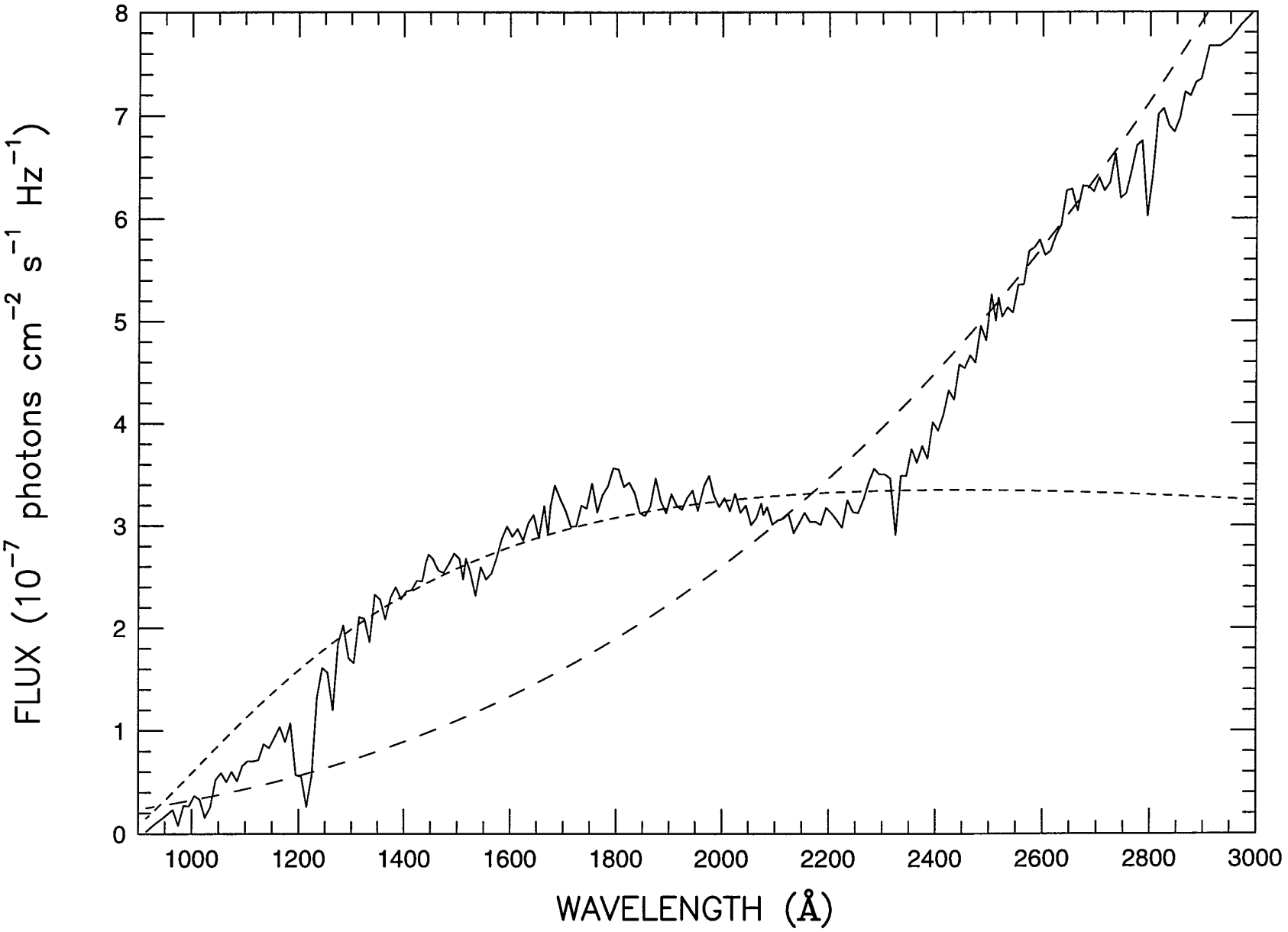
FLUX (10^{-7} photons cm^{-2} s^{-1} Hz^{-1})
0
1
2
3
4
5
6
7
8
1000
1200
1400
1600
1800
2000
2200
2400
2600
2800
3000
WAVELENGTH (Å)

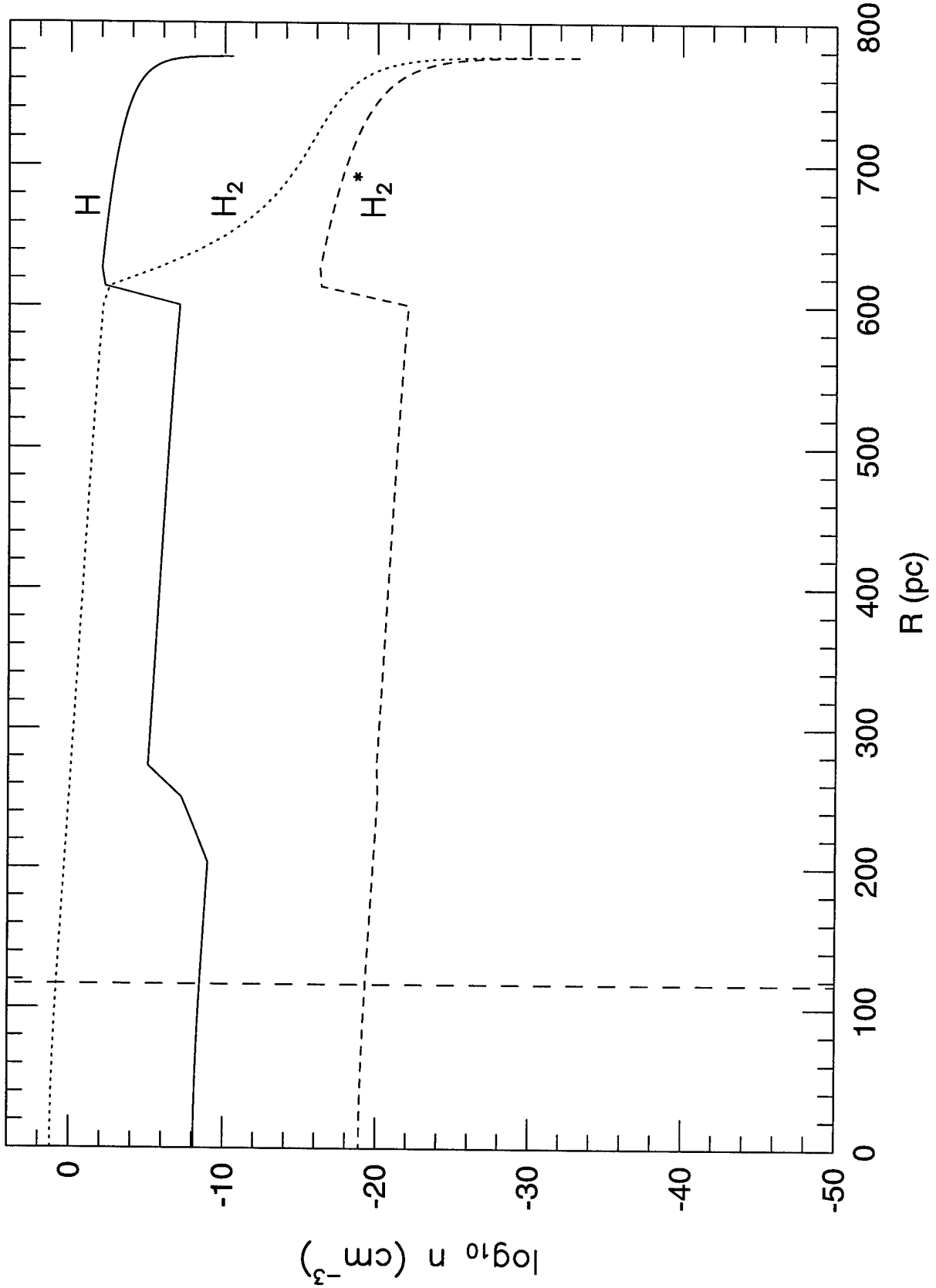
figure 10
H
H_2
H_2^*
0
-10
-20
-30
-40
-50
$\log_{10}$ n (cm^{-3})
0
100
200
300
400
500
600
700
800
R (pc)

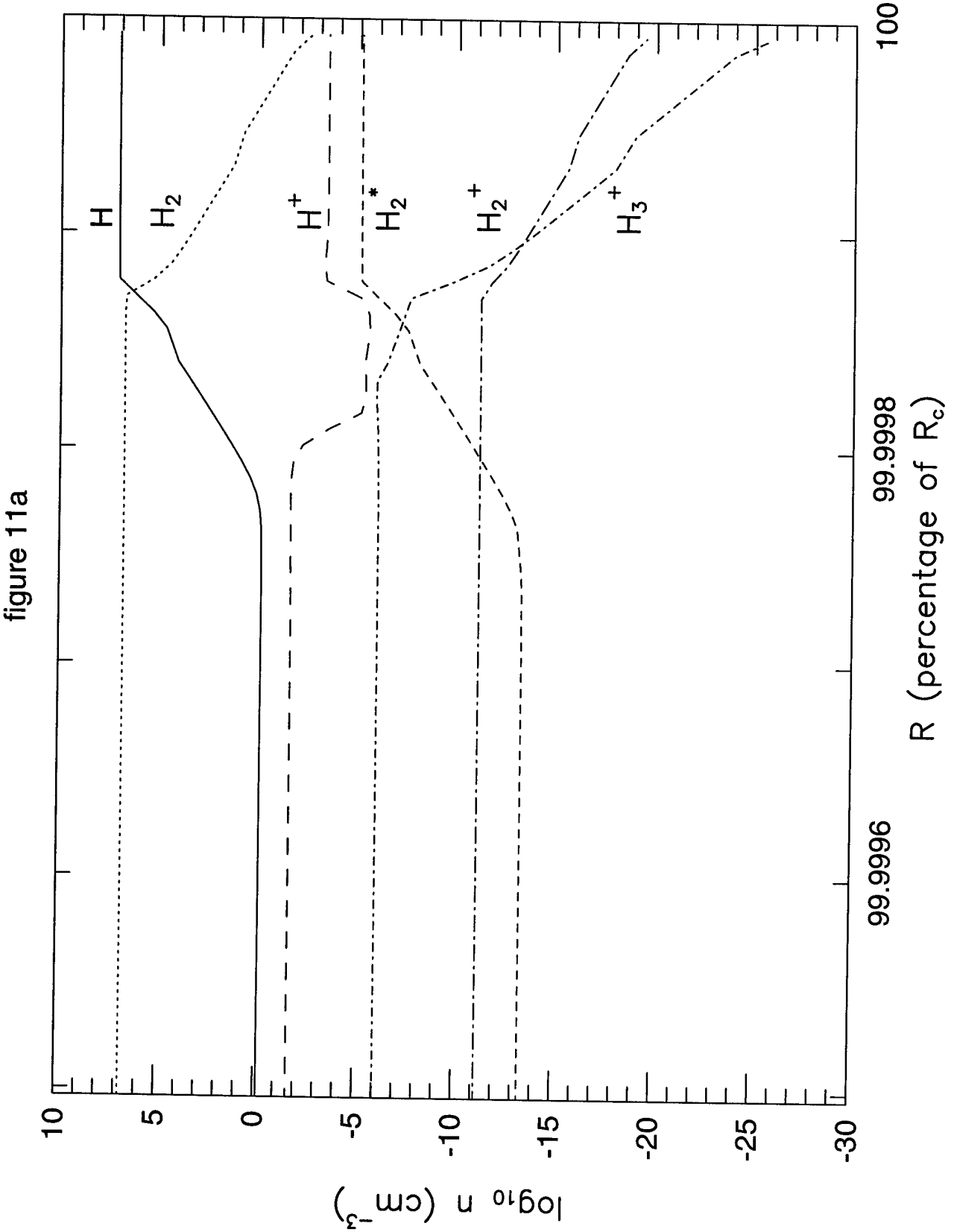
figure 11a
H
H_2
H^+
H_2^*
H_2^+
H_3^+
10
5
0
-5
-10
-15
-20
-25
-30
$\log_{10}$ n (cm^{-3})
99.9996
99.9998
100
R (percentage of R_c)

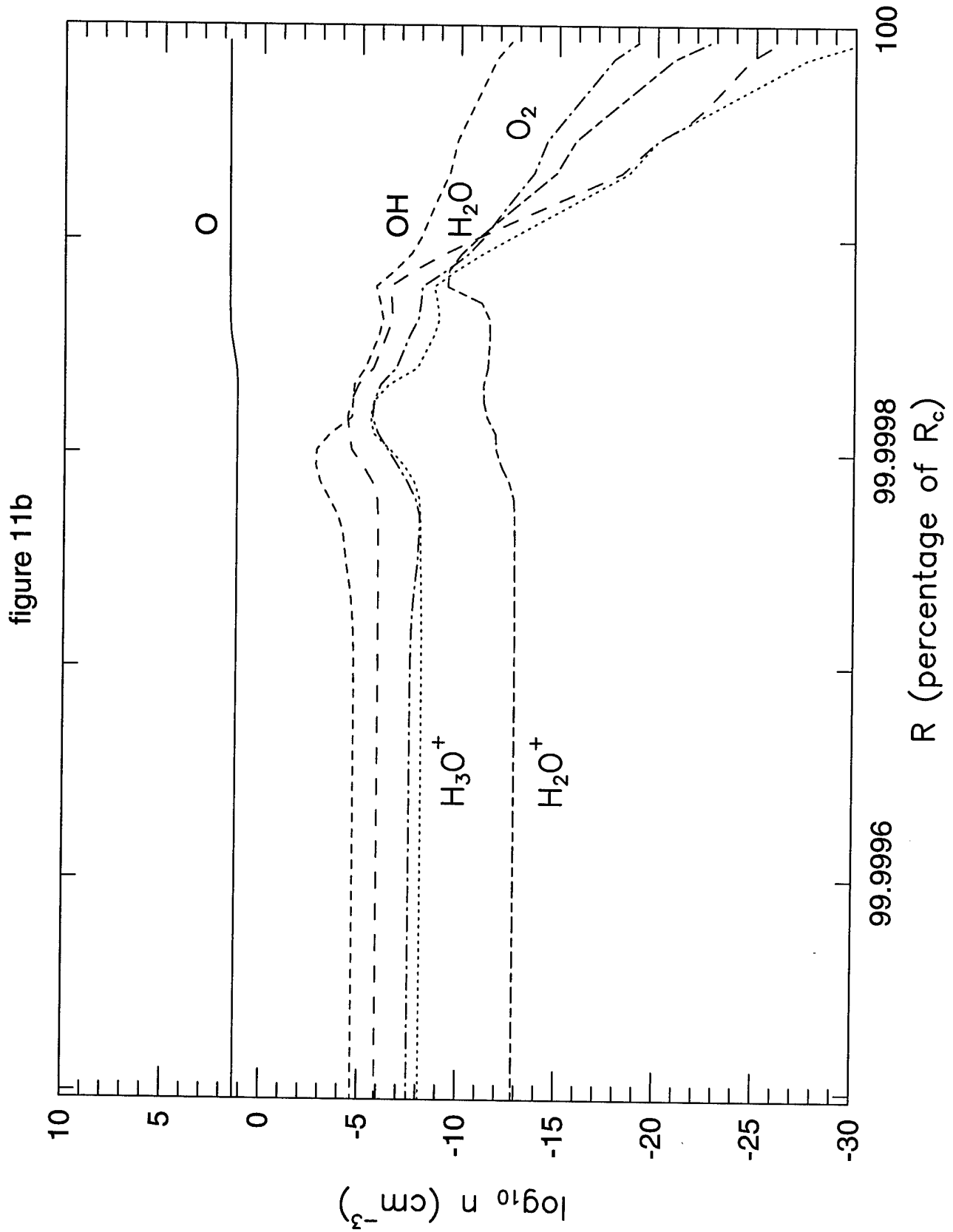
figure 11b
log10 n (cm⁻³)
10
5
0
-5
-10
-15
-20
-25
-30
99.9996
99.9998
100
R (percentage of Rc)
O
OH
H2O
O2
H3O+
H2O+

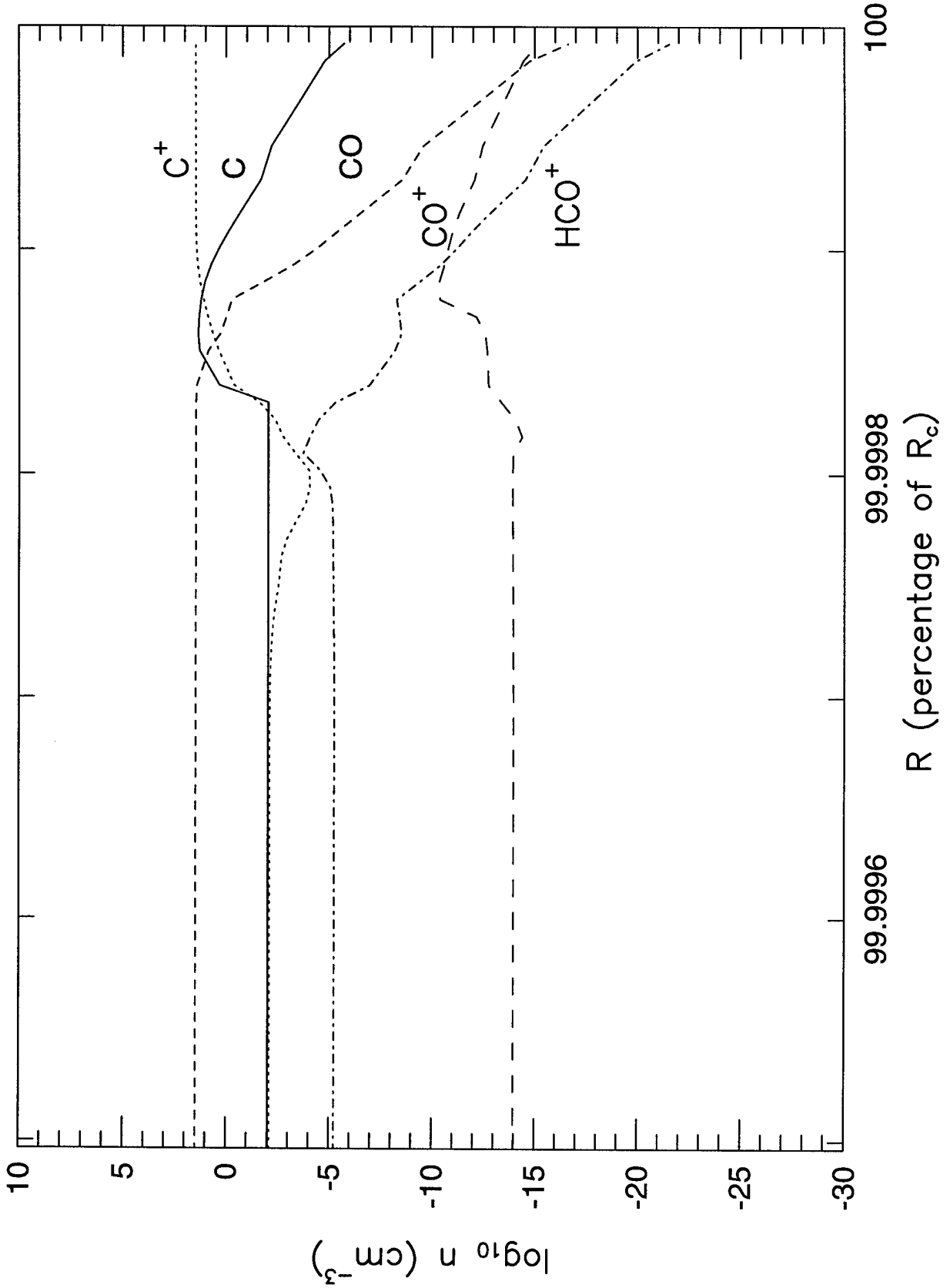
figure 11c
10
5
0
-5
-10
-15
-20
-25
-30
log10 n (cm-3)
99.9996
99.9998
100
R (percentage of Rc)
C+
C
CO
CO+
HCO+

figure 12a

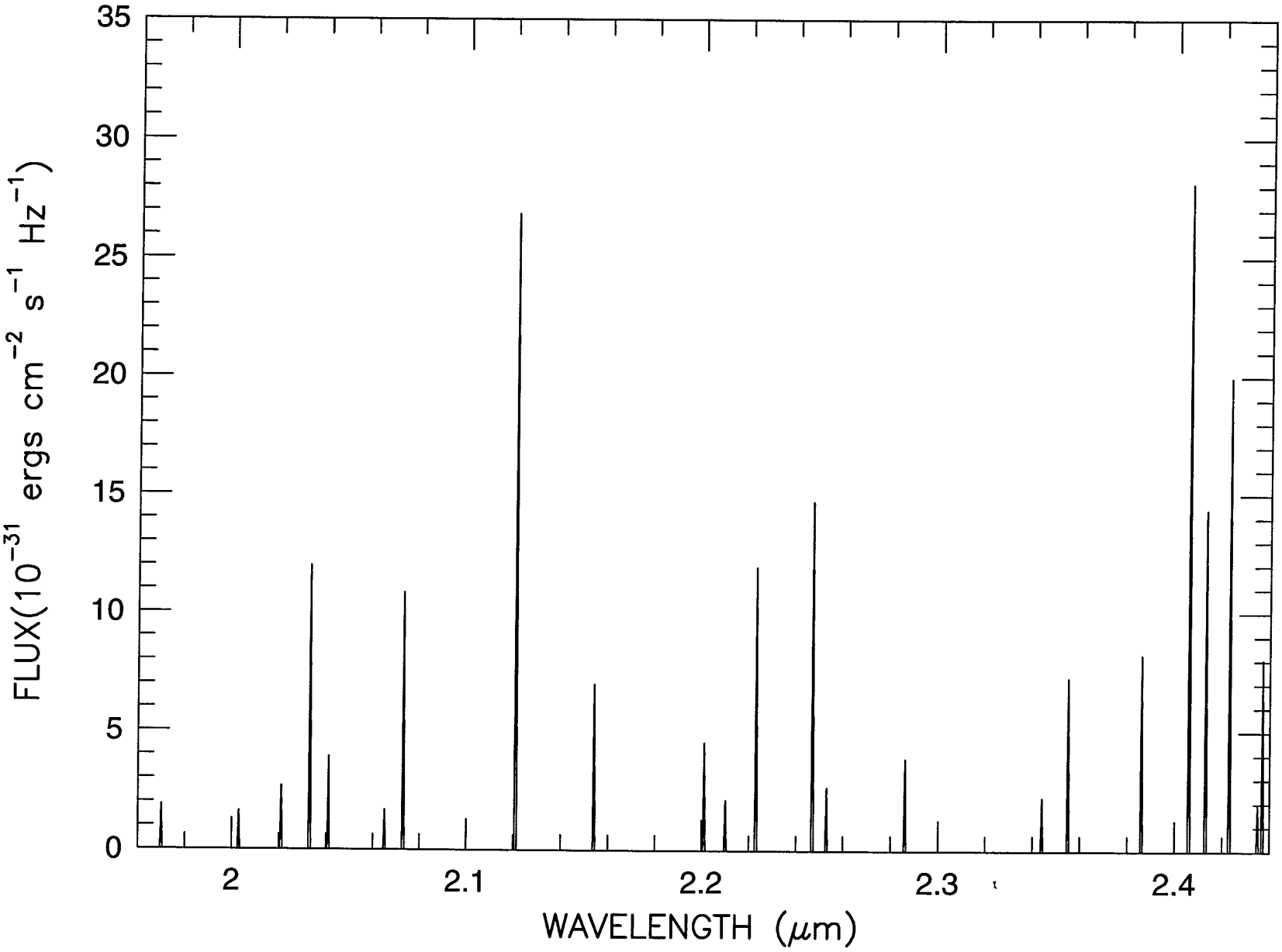
35
30
25
20
15
10
5
0
FLUX(10^{-31} ergs cm^{-2} s^{-1} Hz^{-1})
2
2.1
2.2
2.3
2.4
WAVELENGTH (μm)

figure 12b

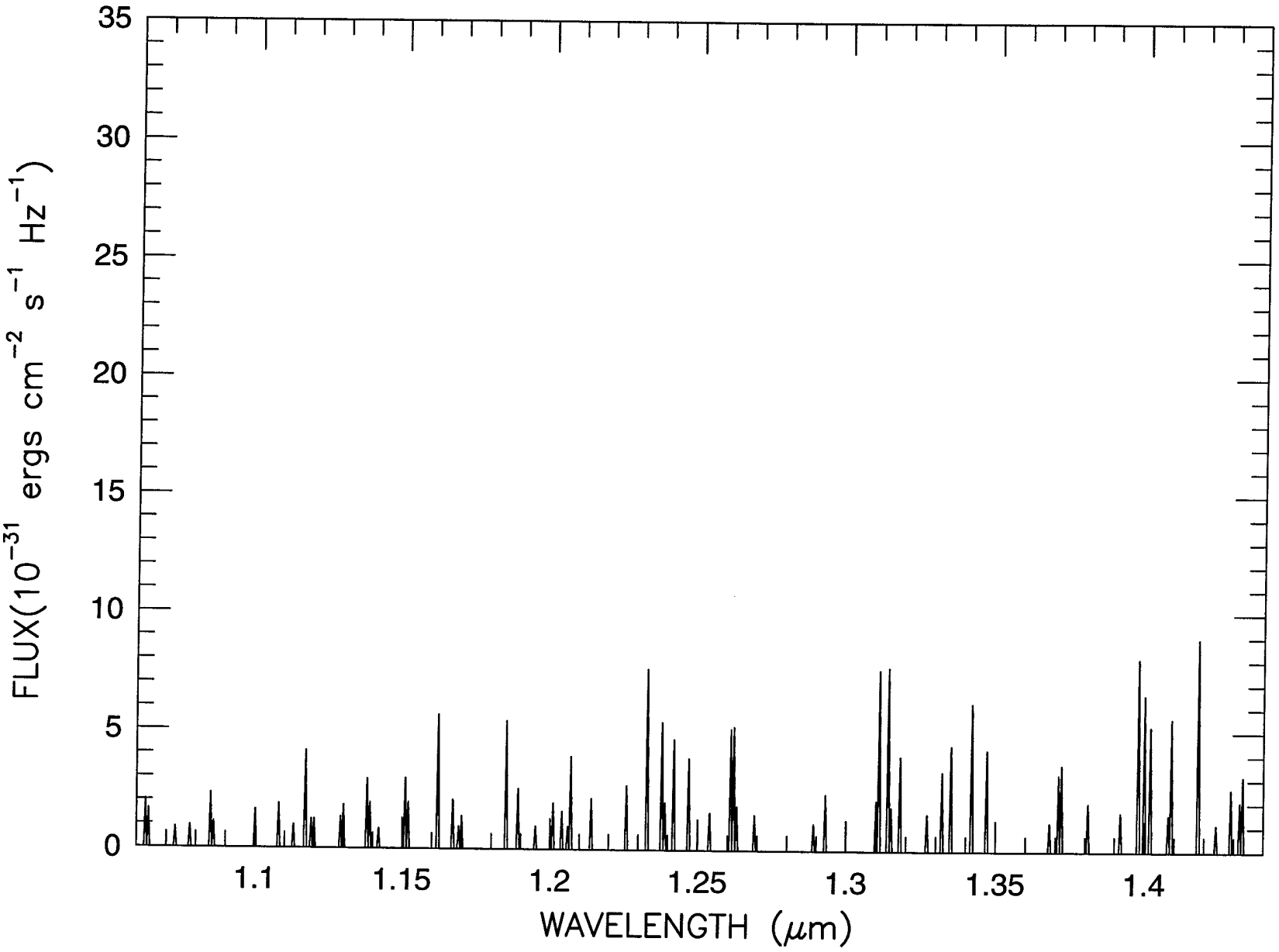
35
30
25
20
15
10
5
0
FLUX(10^{-31} ergs cm^{-2} s^{-1} Hz^{-1})
1.1
1.15
1.2
1.25
1.3
1.35
1.4
WAVELENGTH (μm)

Thesis Abstract, References and Data

ABSTRACT

High-precision velocity measurements of faint individual stars in the Galactic dwarf spheroidal galaxy Draco indicate that the mass-to-light ratio in this system may be as high as ~ 100. Various possible forms of dark matter have been proposed for this class of objects, but a more recent analysis based on the Projected Mass Estimator technique seems to suggest that the non-luminous mass is distributed and may trace the stellar population. Here, we examine in detail the possible contribution of H_2 to the dark matter content of Draco and conclude that most of its mass may be in the form of $\sim 10 - 100\ M_\odot$ H_2 clouds if the typical dust grain size is at least ~ 90 times larger (i.e., $\gtrsim 48\ \mu$m) than in our galaxy. This may be consistent with the fact that the dominant dust destroying mechanisms (e.g., supernova shocks) that suppress the average grain size in the galactic plane are absent in typical dwarf Spheroidals. Thus the absence of dynamical processes (such as supernova explosions) that would normally induce massive star formation (which is non-existent in Draco) may also account for the large grain size. The lack of any observed extinction in this system would be consistent with the very low areal covering fraction ($\sim 0.1 - 1\%$) of the clouds. We show that the predicted H content in Draco is then below current 21 cm detection limits, and that even NICMOS on HST would be hard pressed to detect the prominent J and K band emission lines of excited H_2.

References

Aaronson, M. & Olszewski, E.W. 1987, in *Dark Matter in the Universe*, ed. J. Kormendy & G.R. Knapp (Reidel: Dordrecht), p. 153.

Allen, C. W. 1973, Astrophysical Quantities, 3rd ed. (London: Athlone Press).

Bahcall, J. N. 1986, Ann. Rev. Astron. Astrophys, 24, 577.

Bahcall, J. N. & Maoz D. 1993, Ap. J. Supp., 88, 53.

Bahcall, J. N. & Soneira R. M. 1981, Ap. J., 246, 122.

Bahcall, J.N. & Tremaine, S. 1981, Ap. J., 244, 805. (BaT)

Binney, J. & Tremaine, S. 1987, Galactic Dynamics, Princeton University Press.

Black, J. H. & Dalgarno, A. 1977, Ap. J. Supp., 34, 405.

Black, J. H. & VanDishoeck, E. F. 1987, Ap. J., 322, 412.

Da Costa, G.S. 1992, in *Stellar Populations of Galaxies*, ed. B. Barbuy & A. Renzini (Kluwer: Dordrecht).

Draine, B. T. 1978, Ap. J. Supp., 36, 595.

Draine, B. T. & Salpeter, E. E. 1979, Ap. J., 231, 438.

Elmgreen, B.G. 1993, Ap. J., 411, 170.

Fazio, G. G. & Eisenhardt, P. 1990, in Observatories in Earth Orbit and Beyond, Ed. Y. Kondo (Dordrecht: Kluwer), p. 193.

Gerhard, O.E. & Spergel, D.N. 1992, Ap. J. Letters, 389, L9.

Gould, R. J. & Harwit, M. 1963, Ap. J. 137, 694.

Habing, H. J. 1968 Bull. Astr. Inst. Netherlands, 19, 421.

Haller, J.W. & Melia, F. 1996, Ap. J., 446, in press.

Heisler, J., Tremaine, S., & Bahcall, J.N. 1985, Ap. J., 298, 8. (HTB)

Hodge, P. W. 1971, Ann. Rev. Astron. Astrophys, 9, 35.

Jeans, J. 1902, Phil. Trans. Roy. Soc. London, A 199, 1.

Jura, M. 1975, Ap. J., 197, 575.

Jura, M. 1977, Ap. J., 212, 634.

King, I.R. 1966, A.J., 71(1), 64.

Knapp, G.R., Kerr, F.J. & Bowers, P.F. 1978, A.J., **83**, 360.

Kurucz, R. L., 1993, Kurucz CD-ROM No 13.

Martin, P. G. 1978, Cosmic Dust, Its Impact On Astronomy (Clarendon Press: Oxford).

Martin, C., Hurwitz, M. & Bowyer, S. 1990, Ap. J., 354, 220.

Martin, C., Hurwitz, M. & Bowyer, S. 1991, Ap. J., 379, 549.

Mateo, M., Olszewski, E.W., Welch, D.L., Fischer, P. & Kunkel, W. 1991, A.J., **102**, 914.

Mihalas, D. and Binney, J. 1981, Galactic Astronomy-Structure and Kinematics, (San Francisco: W. H. Freeman and Company).

Mould, J., et al. 1990, *Ap. J. (Letters)*, **362**, L55.

Olszewski E. 1994, private communication.

Paltoglou, G. & Freeman, K.C. 1987, in *Structure and Dynamics of Elliptical Galaxies*, ed. T. de Zeeuw, (Reidel: Dordrecht), p. 447.

Paresce, F. & Jakobsen, P. 1980, Nature 288, 119.
Prasad, S. S. & Huntress, W. T. Jr. 1985, Ap. J. Supp., 43, 1.
Pryor, C. & Kormendy, J. 1990, A.J., 100, 127. (PK).
Roberge W. G. 1981, Topics in the Physics of Interstellar Clouds, Ph.D. Dissertation, (Ann Arbor: UMI).
Rogerson, J.B. et al. 1973, Ap. J. Letters, 181, L97.
Savage , B. D. & Mathis J. S. 1979, Ann. Rev. Astr. Ap., 17, 73.
Scott, E.H. & Rose, W.K. 1975, Ap. J., 197, 147.
Shull, J. M. & Becwith, S. 1982, Ann. Rev. Astron. Astrophys., 20, 163.
Spitzer, L. 1978, Physical Processes in the Interstellar Medium (New York: John Wiley & Sons).
Sternberg, A. & Dalgarno, A. 1989, Ap. J., 338, 197.
Stetson P. B. 1980, A. J., 85, 387.
Strobel & Lake 1994, Ap. J. Lett., 424, L83.
Thompson, R. 1996, private communication.
Tielens, A. G. G. M. & Hollenbach, D. 1985, Ap. J., 291, 722.
VanDishoeck, E. F. & Black, J. H. 1986, Ap. J. Supp., 62, 109.
Young, P.J. 1980, Ap. J., 242, 1232.
Zinn, R. 1978, Ap. J., 225, 790.

Thesis Data

Author: Marcus A. Boyd
Title: The Hydrogen Contribution to the Dark Matter in Draco
Rank: Captain
Service Branch: USAF
Date: 1996
Number of Pages: 55
Degree Awarded: Master of Science (MS)
Name of Institution: University of Arizona